Unit Commitment with Sub-hourly Generation and Ramp Constraints for Systems with Significant Renewables

Md Salman Nazir

Master of Engineering

Department of Electrical and Computer Engineering

McGill University

Montreal, QC

July 2015

A thesis submitted to McGill University in partial fulfillment of the requirements of the degree of

Master of Engineering

Abstract

With significant growth in wind generation in the recent years, addressing the challenges related to integration of wind into power systems has become an important area of research. In power systems, generation and demand must always balance. There must also be enough reserve generation capacity to meet fluctuations in load and renewable sources. Based on the 24 hour demand and wind forecasts, system operators schedule the generation and reserve by solving a day ahead Unit Commitment (UC). During operations, the generators must respect the trajectory limits set by UC. While having too much reserve is expensive, having less of it is risky since increased load shedding or wind curtailment may occur. Moreover, due to high penetration levels of renewables, thermal generators (Natural gas/ coal/ combined cycle plants) experience frequent 'cycling' (ramp up or down of their power outputs) rather than operating at stable levels. The increased cycling has detrimental effects on the long term operational costs (order of millions) due to thermal stress and fatigue.

While several recent studies address the above mentioned challenges, the focus has mainly been on hourly to daily operations, primarily since the UC traditionally deals with hourly time steps. However, at high penetration of renewables, several issues may arise in the sub-hourly time frame, mostly due to large wind ramps and increased sub-hourly ramping needs from thermal generators. Therefore, the thesis deals with the sub-hourly issues by addressing three main areas: (1) A detailed characterization of intra-hour wind behavior, (2) revisiting the sub-hourly ramp behavior and associated costs of the thermal generators, and (3) Incorporating the

sub-hourly wind and thermal generator ramp behavior in the mixed integer linear formulation of the UC.

To characterize wind variability in the intra-hour time frame, a general methodology is presented and its use is demonstrated on 5-minute interval wind power datasets from utilities. We noticed how wind distributions vary depending on generation levels and find the best fit distributions. Since balancing wind could call for significant cycling operations from thermal generators, we also consider the sub-hourly ramping characteristics of generators. To analyze the cost of cycling, a detailed review of findings from operational experiences and research studies has been presented.

Finally, the thesis presents how the sub-hourly ramp characteristics of wind and thermal generators should be incorporated into power systems scheduling applications so that enough flexible capacity is allocated to deal with wind variability. Several implications of these sub-hourly modeling inside UC, such as avoiding dependence on stochastic programming and having access to intra-hour flexible capacity limits, are demonstrated through case studies.

Résumé

En raison de la croissance de la production d'énergie éolienne au cours des dernières années, la recherche sur la façon d'intégrer cette énergie dans les grands réseaux électriques est devenue très importante. Dans les réseaux électriques classiques, la production et la demande doivent toujours être en équilibre. Étant donné l'incertitude et la variabilité dans le niveau de production éolienne découlant des changements d'intensité des vents, l'opération des réseaux à forte pénétration éolienne représente un défi. En amont de l'opération du réseau, on doit planifier suffisamment de capacité de production ayant les caractéristiques dynamiques adéquates pour équilibrer les fluctuations de l'énergie éolienne.

Avec des prévisions horaires de la demande et l'énergie éolienne, le gestionnaire de réseau effectue une planification de l'arrêt-démarrage (PAD) des unités de production classiques (thermales et hydrauliques). Le tout se fait afin de répondre aux niveaux de charge nette (demande moins production éolienne) prévus et à d'autres critères de fiabilité tel que les niveaux de réserves opérationnelles. Lors des opérations en temps réel, les unités de production reçoivent leurs consignes de production. Celles-ci doivent respecter les limites de trajectoires fixées par la PAD. De plus, avec les niveaux élevés de production éolienne, les unités de production thermiques peuvent être fortement sollicités afin d'équilibrer les variations de la charge nette. On s'attend ainsi à des variations fréquentes des niveaux de production tant vers le haut que vers le bas. La fréquence et l'amplitude de ces variations ont des effets néfastes sur les coûts opérationnels à long terme en raison des stress thermiques accrus associés aux variations de niveau de production.

Cette thèse adresse les défis associés aux variations de puissance de la charge nette et leur intégration dans les problèmes de PAD. On y introduit des contraintes et décisions afin de refléter l'importance des variations intra-horaire de la charge nette, généralement négligées dans les problèmes de PAD en présence d'une forte pénétration d'énergie éolienne. Spécifiquement, cette thèse aborde :

(1) Une caractérisation détaillée de la variabilité de l'énergie éolienne intra-horaire,

(2) Le comportement des rampes de production intra-horaire et l'analyse des effets sur les unités de production thermiques, et

(3) L'intégration des variations intra-horaires de l'énergie éolienne et les rampes de production thermique dans la formulation mathématique des problèmes de PAD.

Nous caractérisons la variabilité de la production éolienne dans le temps à l'aide de données empiriques. Nous remarquons que les distributions de la variabilité de l'énergie éolienne varient en fonction des niveaux de production. Nous considérons également les caractéristiques de rampe intra-horaire nécessaires de la part des unités de production thermique.

Enfin, la thèse présente comment les caractéristiques de variabilité intra-horaire de l'énergie éolienne et des limites dynamiques des unités de production thermiques devraient être incorporées dans les PAD. Ainsi, nous optimisons la capacité de production flexible pour faire face à la variabilité dans l'énergie éolienne. Nous présentons plusieurs exemples pour démontrer notre méthodologie.

Acknowledgements

First and foremost, I would like to thank my supervisor, Professor François Bouffard, for many insightful conversations during the development of the ideas in this thesis, for providing detailed feedback on my work and most importantly for coaching me to develop my research skills. He has been a true mentor throughout the years I have known him and worked with him.

Also, I would like to thank to Professor Francisco Galiana, my undergraduate thesis supervisor, for inspiring me to step into the exciting field of power systems. Thanks to Professor Doina Precup for sharing her insights and many helpful discussions during my machine learning course project. Thanks to all of my fellow students at the Power Lab, Mostafa, Ali, Amir, Hussam, Navdeep, Debi Prasad, Diego and Omar for making the stay at McGill's Power Group so special. Thanks to Alexandre, David, Lisa, and other fellow colleagues at CanmetENERGY, Natural Resources Canada for supporting my education by providing me with great deal of flexibility during the time I had been working and studying together.

For financial support, I thank the Department of Electrical and Computer Engineering at McGill University for supporting my education through fellowships. Thanks to Hydro-Québec for awarding me the prestigious Masters Fellowship in Engineering.

I would also like to thank to my parents and my family in Bangladesh for being supporting of my higher education even when it required me to live half a world away from them.

Finally, a special thanks to my wife, Asmita, who has always been by my side and provided me with unconditional support, love and encouragement.

Table of Contents

List of Tables

List of Figures

Acronyms

UC	Unit Commitment
SCUC	Security-constrained unit commitment
WVAR	Wind variability
SKL	Skew-Laplace
PSD	Power spectral density
ISO	Independent system operator
BPA	Bonneville Power Administration

List of Symbols

Indices

t	Index of hours in a day, 1 to 24
ϕ	Index of intra hour segments, 1 to 6
i	Index of generators

Parameters

$\tau(\phi)$	Duration of sub-hourly segment ϕ. Here 10, 20, ..., 60 minutes
T	Planning period (24 hours)
w_{ins}	Installed wind capacity, in MW
$w_{t\phi}^{\text{var}-up}$	Upward wind ramp limit at hour t and sub-hourly interval $\tau(\phi)$, MW
$w_{t\phi}^{\text{var}-dn}$	Downward wind ramp at hour t and sub-hourly interval $\tau(\phi)$, MW
$w^{\text{var}-up-5\text{min}}$	Upward wind ramp limit over a 5 minute interval, MW
$w^{\text{var}-dn-5\text{min}}$	Downward wind ramp limit over a 5 minute interval, MW
w_t^f	hourly wind generation forecast, MW
$g_i^{\max}$	Maximum generation of unit i, MW
$g_i^{\min}$	Minimum generation of unit i, MW
$r_i^{up-rate}$	Upward ramp rate limit of unit i, MW/min
$r_i^{dn-rate}$	Downward ramp rate limit of unit i, MW/min
$R_{i\phi}^{up}$	Up ramp limit provided by generating unit i at hour t and sub-hourly interval $\tau(\phi)$, MW

$R_{i\phi}^{dn}$	Down ramp limit provided by generator *i* during hour *t* and sub-hourly interval $\tau(\phi)$, MW
A_i	Fixed cost for generating unit *i*, \$/h
B_i	Incremental cost of generation of generating unit *i*, \$/MWh
RC_i	Incremental cost of ramping of generating unit *i*, \$/MWh
α, β, μ	Parameters of the skew-Laplace distribution

Variables

u_{it}	Unit commitment decision variable
g_{it}	Total power output of generating unit *i* at period *t*, MW
$g_{it\phi}^{s}$	Generator level of unit *i* during hour *t* and sub-hourly interval $\tau(\phi)$, MW
$r_{it\phi}^{up}$	Up reserve capacity provided by generator *i* during hour *t* and sub-hourly interval $\tau(\phi)$, MW
$r_{it\phi}^{dn}$	Down reserve capacity provided by generator *i* during hour *t* and sub-hourly interval $\tau(\phi)$, MW
C_i	Cost of generation for unit *i* , \$/day
TC	Total cost of UC, \$/day
w_t^g	Wind power output at hour *t*, MW
w_t^s	Wind curtailed or spilled at hour *t*, MW
$g(x;\alpha,\beta,\mu)$	Probability distribution function of skew-Laplace distribution

Chapter I Introduction

I.A. Context and Motivation

Wind power has experienced tremendous growth over recent years and is expected to continue to grow. This rapid growth can mainly be attributed to clean energy mandates to reduce emissions and the cost-effectiveness compared to other forms of fossil fuel based electricity generation sources.

Worldwide wind power capacity has reached 336 GW in June 2014 (Compared to 47.6 GW in 2004), and wind energy production was around 4% of global electricity usage, and growing rapidly. China (91,412 MW), USA (61,091 MW), Germany (34,250 MW), and Spain (34,250 MW) are currently among the leading countries by cumulative capacity installed. In Canada, this amounts to 7803 MW [1].

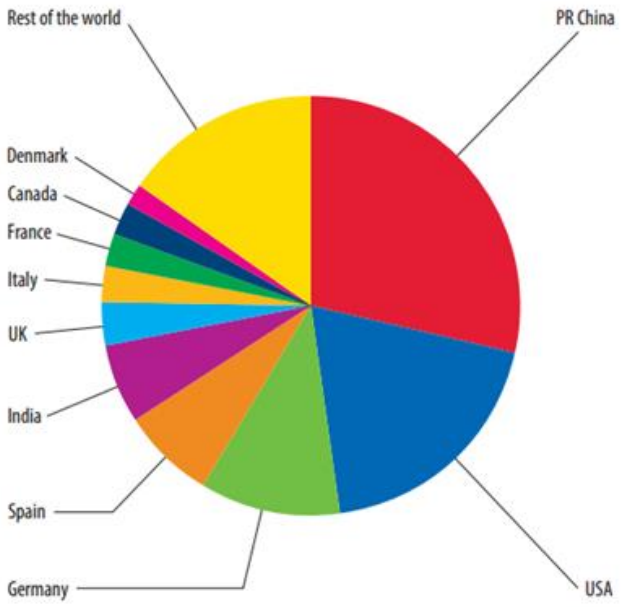

Figure 1. Wind installed pie chart by countries [1].

In Europe, several countries, such as Denmark, Portugal, Spain, the Republic of Ireland and Germany have reached high penetration levels of wind. On an annual basis, in 2014, 39% of Denmark's annual energy was produced by wind. On a daily basis, wind power can often contribute to more than 50% of the instantaneous power in several systems that have integrated high wind capacity.

While these high penetration levels are encouraging, many studies are being carried out to quantify the impact of high wind power generation on power systems, as well as to addressing challenges associated anywhere from 10% to 50% penetration levels [2]-[5]. Because instantaneous electrical generation and consumption must remain in balance, uncertainty and variability associated with renewable sources such as wind can present substantial challenges to incorporating large amounts of wind power into a grid system. System operators need to schedule enough of the appropriate dispatchable resources—essentially controllable generation, storage and demand response—ready to counteract the unexpected and variable nature of wind at any time during real time operation [2], [6]. For managing uncertainty and variability, modeling of wind behavior has therefore become an important task for system operators and other stakeholders.

I.B. Need for Intra-hour Wind Variability Modeling

While several studies focus on hour-to-hour analysis of wind power behavior, wind generation is not just random from hour-to-hour [7]. Deployment of available reserve capacity during respective frequency regulation phases (primary, secondary and tertiary) are sub-hourly events and hence the importance of sub-hourly analysis of wind plays a critical role [6].

The authors in [2] described a typical wind farm indicating ramp rates of up to 4.4% of total capacity per second implying a large burden on fast deployment reserves. In fact, an empirical

analysis of increasing wind penetration in the Pacific Northwest area of the United States demonstrated that reserve requirements increased with the square of installed wind capacity, and the need for total reserve capacity doubled after just 2500 MW of installed wind capacity. Another recent study for the Public Service of Colorado (PSCO) [7] area shows that there are more occurrences of up-ramps compared to down-ramps. The more strict the ramp definition (i.e., the larger the threshold), the higher the percentage of up-ramps compared to down-ramps. For the case of variability observed over a 60-minute interval, the percentage up-ramps versus down-ramps were at 58%, 69%, and 87%, respectively. The results also indicate that a ramp greater than 25% of total generation in PSCO is likely to occur almost once per day, and when it occurs it may happen very rapidly and then potentially have a large impact on intra-hour operations. For example in the BPA (Bonneville Power Administration, USA) system, upward ramps of up to 53% of total wind generation capacity (and downward ramps of 42%) within 60 minutes were observed in 2009 [8]. These observations warrant a rigorous analysis to characterize intra-hour wind power variability is essential.

While it is widely agreed that probabilistic models for wind power variability would be immensely useful, the main challenge in the detailed analysis of wind power characteristics remains in the availability of wind power time series data with the appropriate sampling rates and required durations [6], [9]. Moreover, most power systems have limited years of operational experience with large wind capacity. This limiting factor led to many studies of wind power uncertainty and variability being confined in the analysis of hour-to-hour variations [2], [7]. Without modeling of intra-hour wind variability, system operators have to base their decisions regarding short term regulation, time and duration of ramp requirements on their judgments or other assertions, which may then lead to sub-optimal planning in the form of higher costs of

operations and increased wind curtailment [6], [11]. A study by Greenpeace [12] points out that if used to its full potential, more accurate forecasting could slash the associated system balancing costs significantly (by nearly 30% for Germany). These forecasts can be improved with improved availability of historical data and better forecasting methods.

I.C. Need for Incorporating Generator Flexibility in Planning Tools

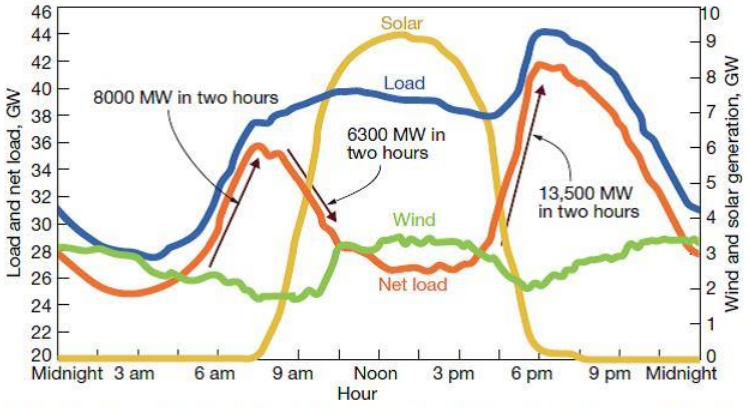

1. Load profile projected by the California Independent System Operator for January 2020 (high-load case) illustrates the challenge facing generators in the state

Figure 2. Projected load and generation behavior in 2020, also known as the 'duck curve' [10]

Figure 2 [10] shows a forecasted scenario of the daily behavior of wind, solar and load in 2020 in California Independent System Operator (CAISO) to demonstrate how large penetration of renewables may require significant flexibility from the rest of the generation mix. With high penetration of renewable resources, the net load (red curve) is the trajectory conventional resources would have to follow. It comprises of a series of ramps of significant magnitude and short duration. It should also be noted that neither wind nor solar peak production coincides with the system peak load. As wind penetration levels reach 10% to 50% of total installed generation capacity, rapid ramps in wind power output can become of significant importance. Generators that are capable of providing such rapid ramps to shadow the wind power variability in the very

short term may be called to be highly flexible [6], [13]. But such flexibility comes at a cost. Typically, generators have to go through increased cycling which can have detrimental mechanical strain effects. In turn, it is reasonable for such flexible assets to seek appropriate compensation. Moreover, from a generation planning perspective, system operators have to ensure that enough flexible plants with the appropriate dynamic characteristics (over a spectrum of time intervals) will be in service when large amounts of wind power are operational. Therefore, the quantification of intra-hour wind variability is also crucial for valuation of such flexibility and for making sure there is enough of it [6].

I.D. Organization and Contribution of the Thesis

To address the above-mentioned challenges, this thesis aims to: (1) Quantify the intra-hour wind variability envelope, (2) Revisit the generator ramp (change of power output levels) characteristics in the sub-hourly time frame, and (3) Integrate the above two models into a power systems scheduling application in a computationally-efficient manner.

Chapter II presents a detailed literature review. Then, in Chapter III, a methodology is presented to analyze intra-hour wind power behavior both time and frequency domains. This analysis leads to a systematic characterization of this variability. Our work goes beyond most of the published literature on wind power variability which generally concerns itself only with hour-to-hour variations. As a second step, we attempt to establish best fit models and corresponding parameters in both domains. In the time domain, since the mean, variance, skewness and kurtosis of time series all convey important messages regarding the average, spread, shape and peakedness of a distribution, we attempt to fit probability density functions (PDF) that can take all these into account and best fit empirical data. In [11], we find that the skew-Laplace distribution, which is a more generalized form of the Laplace distribution, can be used most

effectively to describe wind variability over given sub-hourly time intervals. We present this finding based on the year-long 2009, 5-minute sampled, wind power data from BPA [8]. We notice that skewness in that 2009 BPA data showed dependence on time duration, well as on time of day and season of the year. In the frequency domain, we show from the Power Spectral Density (PSD) estimate of the 2009 BPA wind data that the average estimated wind power variability falls as $f^{-2.4}$ over the range of frequencies corresponding to 10 minutes up to several hours.

Afterwards, we present a systematic characterization of sub-hourly wind behavior from operational data rather than from capturing only the absolute changes in magnitudes, standard deviations and ramp durations. Such characterization should help with designing better intra-hour operational protocols and practices in systems with large wind power penetrations. In turn, system operators should be in a better position to increase the likelihood of successfully integrating large amounts of wind energy without significantly increasing system costs associated with scheduling of extra reserve, more frequent cycling of traditional generators and its associated thermal fatigue effects, as well as potentially higher emissions [6], [14].

Unit commitment (UC) is known as the key day-ahead power systems planning tool whose goal is to schedule enough electricity generation and reserve capacity to meet demand reliably and economically [15], [16]. Chapter II provides a detailed review of a number of adaptations of the Unit Commitment that have been proposed to deal with the uncertainty and the variability of wind. However, due to its usual hourly time steps, intra-hour phenomena are not modeled explicitly and hence may lead to sub-optimal decision in the real-time operation. Therefore, we identify additional intra-hour constraints that need to be incorporated in the UC to capture sub-hourly wind and generation ramp behavior, modeling of which has been detailed in Chapter III.

Additionally, these constraints are integrated in the mixed integer linear formulation of the unit commitment with minimal additional complexity.

Chapter IV presents detailed case study results using BPA data and a three generator test system. Finally, Chapter V presents conclusions and suggestions for future extensions.

Chapter II Literature Review

II.A. Probabilistic Modeling of Wind Behavior

While wind power variability is often assumed to follow a normal distribution by invoking the central limit theorem [5], [17], recent studies show that this assertion is not necessarily true and hour-to-hour wind power variability can be modeled much better with a Laplace distribution [18]. This is understandable since invoking the central limit theorem would be justifiable only if the aggregate wind output levels were very high and wind farms were not located diversely across a large geographic area. But instead in most cases, wind farms cannot be placed in such a random manner and thus outputs have high degree of correlation. In the BPA system, for example, this is obvious. Moreover, at times when the variations are low either due to generation output levels being low or due to considering change within a very short time duration, invoking central limit theorem cannot be justifiable.

In [18], the author employed parametric and non-parametric evaluation techniques on several probability distributions to determine their suitability as models of hourly variability. Using the Bonneville Power Administration (BPA), the Electric Reliability Council of Texas (ERCOT) and the Midcontinent Independent System Operator (MISO) wind power output data, the author carried out his analysis for hourly timeframes and showed that beta distributions are the most appropriate probabilistic models for aggregate wind power outputs, while Laplace distributions are the most appropriate probabilistic models for wind power variability.

In Chapter III of this thesis, we present a methodology for analyzing the intra-hour variability and subsequently in Chapter IV we present results on empirical data from BPA.

II.B. Unit Commitment with Significant Wind Power Generation

Several approaches to address the challenges in integrating significant wind is presented in recent literature – a detailed literature review is available in [22]. Broadly, the formulations can be classified either as deterministic or stochastic. In [23], generator outages, load, and wind forecasting errors are taken into consideration when determining the required amount of system reserves in a deterministic setting. A reliability target is defined before calculating the reserve requirement for the system. However, pre-defining a reliability target may be difficult and may differ for different systems. A rolling-horizon commitment method is used to schedule the thermal units in [26] to incorporate the possibility of trajectory revisions due to updated forecasts.

Ortega-Vazquez and Kirschen [24] proposed a Monte Carlo simulation based method to calculate the optimal amount of spinning reserve requirements. The method is based on the cost/benefit analysis method proposed in the authors' previous work [25]. The authors concluded that an increased wind power penetration does not necessarily require larger amounts of spinning reserve. However, this conclusion cannot be generalized since it depends heavily on the assumptions of the study, its underlying models, as well as the generation portfolio and load profiles.

Bouffard and Galiana [17] proposed a stochastic unit commitment model to integrate significant wind power generation while maintaining the security of the system. The wind uncertainty is modeled by a scenario tree provided that the wind forecasting error is subject to a normal distribution. The reserve requirements are determined implicitly by simulating the wind power realization in the scenarios rather than being pre-defined. Wind curtailment and load shedding are also allowed as last resort potential control actions. The authors acknowledged in

their paper that the problem is prone to dimensionality issues when large systems and multiple scenarios need to be considered.

Ruiz et al. also [27] also proposed a stochastic formulation to manage uncertainty in the unit commitment problem. The stochastic alternative to the traditional deterministic approach can capture sources of uncertainty and define the system reserve requirement in the scenarios. In [28] authors analyze the economic valuation of reserves by considering network constraints and realistic scenarios. However, most of these work on UC with wind rely on modeling wind forecasting errors as a normal distribution, and not incorporating the intra-hour wind variability characteristics. Another important aspect that is not considered in all this work is the detailed treatment of the intra-hour ramping behavior of wind and thermal generators, which can have important implications on the hourly and daily generation scheduling and dispatch decisions.

II.C. Ramp Rates and Cycling Costs

While traditional UC assumes linear ramping from generators during sub-hourly intervals, Figure 3 shows a range of sub-hourly start-up ramp profiles for the same generator [29]. It shows how a combined cycle power plant is capable of cycling and can follow many different trajectories in the sub-hourly time frame and offer higher flexibility compared to conventional thermal power plants. However, following a fast ramping trajectory needs to be backed by sufficient incentives since it can lead to increased wear and tear of the generation equipment [31], [32], [33].

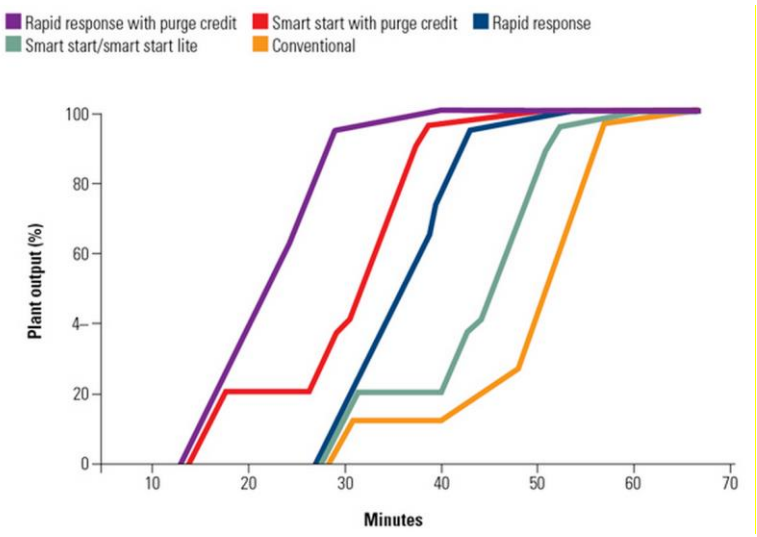

Figure 3. Range of generator ramp profiles during start up [29]

II.C.1. Exposure to Increased Thermal Stress:

When thermal generators ramp up, they reach very high temperatures (above $400\,^{\circ}C$) and pressure levels, which go through fast gradients. Similarly temperature drops rapidly (at specific ranges) during the ramp down process. Typical start-up and shut-down curves from generator operational data are shown in Figure 3 [30]. Mechanical stress is induced in a body when some or all of its parts are not free to expand or contract in response to changes in temperature. In most continuous bodies, thermal expansion or contraction cannot occur freely in all directions due to geometry, external constraints, or the existence of temperature gradients, and so stresses are produced.

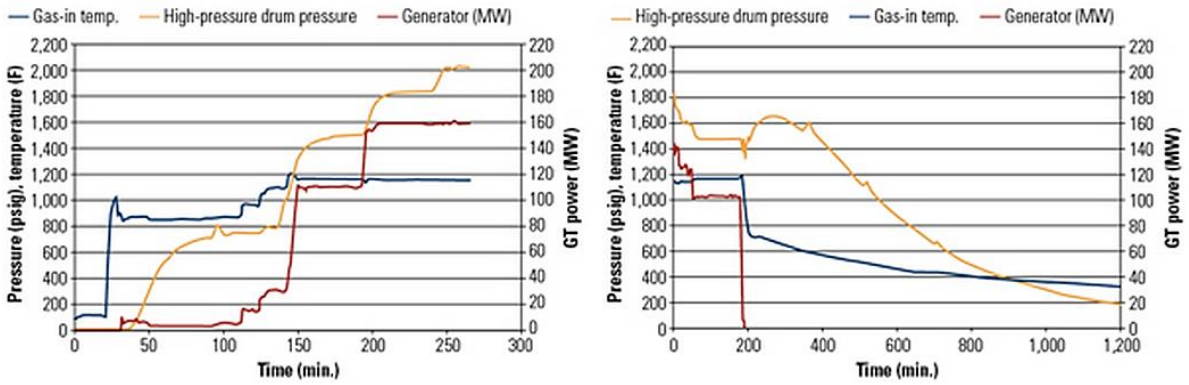

Figure 4. Generator temperature and pressure curves during start up and shut down [30]

II.C.2. Exposure to Cyclic Fatigue:

By far the most common problem experienced as a result of cycling is thermal fatigue damage [31]. Fatigue is the structural damage that occurs when a material is subjected to cyclic loading, i.e. repeated heating and cooling. If the loads are above a certain threshold, microscopic cracks will begin to form at the metal surface of the generator equipment. Eventually a crack will reach a critical size, and the structure may suddenly fracture. The shape of the structure will significantly affect the fatigue life. Thermal stress below elastic limits will not lead to fatigue effects but macroscopic cracks may appear on the turbine rotor surface if the elastic limits are violated frequently [31], [32]. Therefore, it is well understood that thermal generators providing frequent cycling can experience cyclic fatigue.

II.C.3. Damage due to Cycling

Increased 'cycling', i.e. starting up or shutting down and varying output in response to change in load levels, of generating units leads to increased costs due to maintenance, heat rate degradation, and higher probabilities of forced outages. For example, due to cycling in combined cycle power plants, heat recovery steam generators (HRSG), steam pipes, turbines and auxiliary components go through significant thermal and pressure stresses, which can cause structural

damages and significantly reduce the life of components. Thus, generators incur additional maintenance costs due to wear and tear damage, unit replacement cost and increased forced outages [31], [33]. The opportunity cost of unforeseen forced outages is huge. Since thermal stress and ramp rates are directly correlated, to maximize plant value, a cost benefit analysis for providing any extra MW of ramping must be carried out carefully by the plant operators.

A detailed study from EPRI [31] finds that the major cost implications of two-shift operations start to appear at approximately three years after changing from baseload. After this time, the cyclic effects of two-shifting begin to cause significant damage to components – a list of components most prone to damages due to cycling is presented in Table I. The report shows that repair and replacement costs of items such as superheater headers and other critical plant components can be extremely high (in the order of millions of dollars).

Table I Plant Equipment Failure due to Increased Cycling

Component	Percentage of Failures due to Cycling
Boiler tubes	33
Headers	83
Superheater tubes	19
Reheater tubes	40
Condenser	38
High pressure heater	70
Low pressure heater	33

II.D. Unit Commitment with Cycling Costs

Overall, a change to operating under cycling conditions should capture the following:

- Increased capital spending for component replacement and unit life shortening
- Increased routine O&M cost from higher wear and tear
- Lower availability as a result of increased failure rate and outage time
- Increased fuel cost from reduced efficiency and non-optimum heat rate

However, the difficulty lies in establishing the degree to which each of these factors is applicable to any specific plant. The plant specific factors can be very influential in modeling the accurate cycling costs. Since these factors are not publicly disclosed by plant operators and manufacturers, system operators might not be able to optimize over these parameters explicitly. As an alternative, in a study by Delson [34], the ramping of thermal generators was scheduled by considering thermal stress equations. It showed how generators can be scheduled to perform stress-limited ramping which would not incur cycling costs. Control techniques that incorporate stress monitoring are available to power plant operators as well [35].

UC formulations incorporating ramping costs and rotor fatigue effects were proposed in [36], [37]. In [44], authors proposed a profit maximization dispatch strategy where a generator chooses from different ramp profiles considering the ramping costs associated with each profile. However, these studies, [36], [37] and [44], do not present a general methodology for establishing such ramping costs. The authors of [14] and [33] analyzed the impacts of wind power on thermal generation unit commitment and dispatch. More recently, [38] presented a UC model where dynamic ramping costs can be taken into account. However, since most of these studies focus on hourly scheduling, more research is needed to capture issues that might arise due to frequent cycling in the sub-hourly time frame.

Chapter III Modeling and Methodology

III.A. Analysis of Wind Variability in the Time and the Frequency Domains

For analyzing short-term wind power variability, we developed a methodology combining with a number of standard tools. Figure 5 presents the tools and flow of data while carrying out the method.

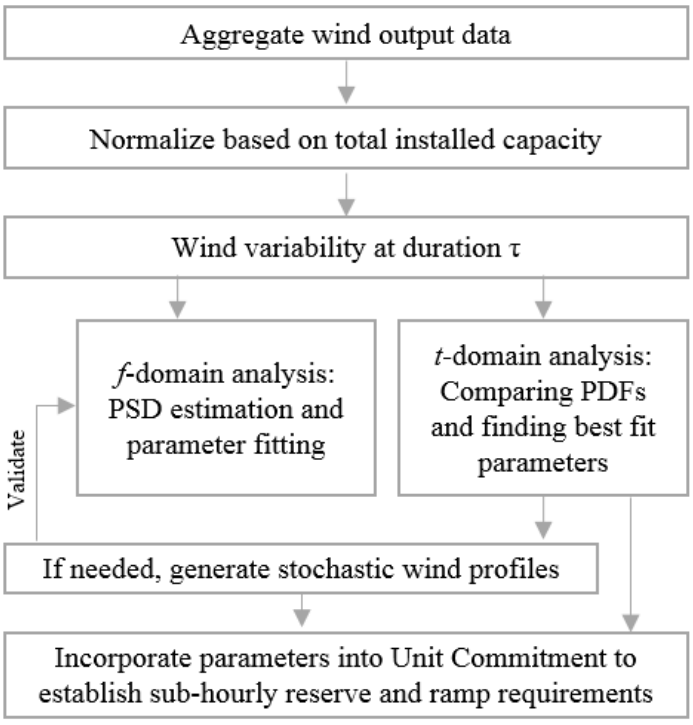

Figure 5. Wind power variability analysis and incorporation into unit commitment

III.B. Data Consideration

For probabilistic modeling of wind characteristics, we test our techniques based on actual field data. BPA has made available through its web page aggregate wind power with five-minute time

resolution backing to 1998 [8]. Such sampling frequency of aggregate wind power data is appropriate for our purposes. Following the techniques presented here, one may attempt to reproduce similar results for other systems worldwide.

Specifically, in the analysis that is to follow, we used the 2009 complete year wind power dataset. These have a resolution of 5 minutes, and all data are for aggregated total real wind power output in the BPA balancing area. There were few missing values which were carefully omitted resulting in a grand total number of samples of 105,108. Individual wind farm data was not available and was not required for this study since we are interested in the aggregate variability that the system operator could experience and its impacts on system behavior. However, our methods can be readily extended to farm or turbine specific analysis if such data are provided.

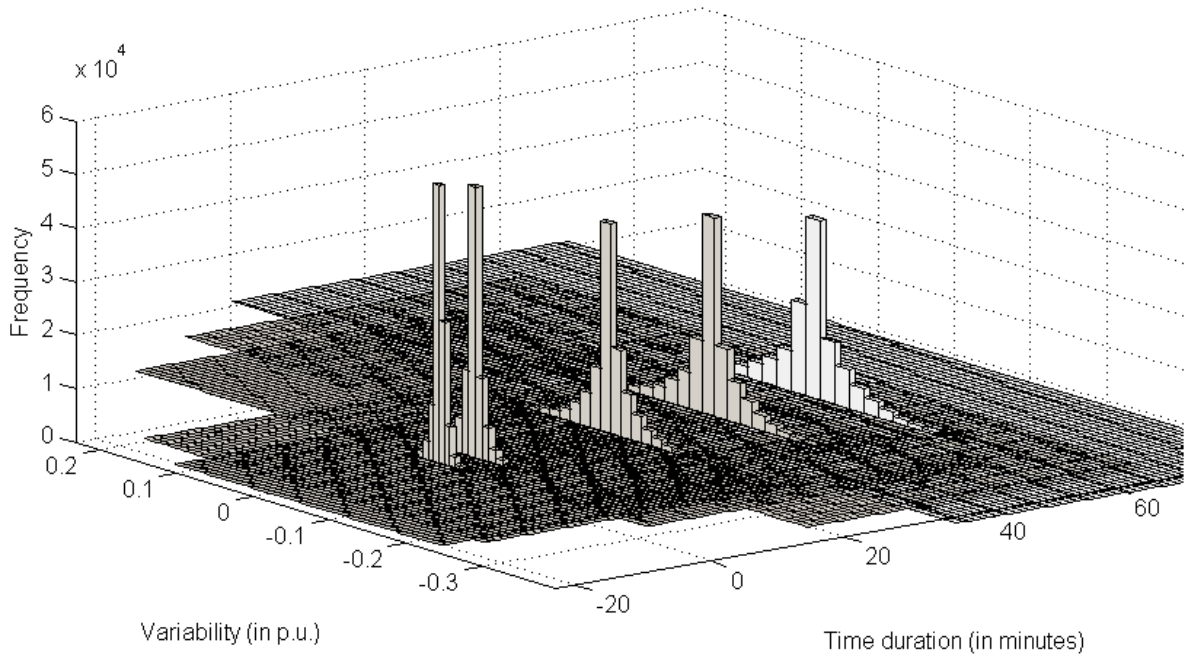

Figure 6. BPA wind variability histograms

The BPA data shows at 01/01/2009 total wind nameplate capacity of 1671 MW, whereas by several additions of 30 through 250 MW size farms, total capacity reached 2617 MW as of 12/16/2009. We normalized the data samples according to the nameplate capacities at corresponding dates so that the variability magnitudes are consistently in per unit.

Data before 2009 was not considered due to insignificant capacity and missing values. Moreover, we assume that the 2009 data has not been affected severely by exogenous factors such as curtailment due to transmission constraints (unlike in ERCOT). In 2010-2013, BPA data shows yet higher wind output; however, it is impossible to assert whether or not recorded wind power levels were affected by transmission-driven curtailment orders. In the case when power data is affected due to curtailments, one could alternatively estimate wind power levels from wind speed data.

III.C. Data Preparation

To analyze the wind power variability over different time intervals, τ = 5, 10, 30, 45, 60 minutes, we need the historical variability corresponding to each τ. These can be obtained from the BPA 5 minute resolution time-series of the aggregate wind output power [8].

Let $x(t)$ be the recorded aggregate wind output power, where *t* represents the time index with 5 minute resolution. $P(t)$ is obtained after normalizing the samples based on aggregate installed capacity at time *t*, $C(t)$.

$$P(t)=\frac{x(t)}{C(t)} \tag{1}$$

To obtain the wind power variability, $\Delta P_{\tau}(t)$, over the specified time duration τ, we use (2);

$$\Delta P_{\tau}(t) = P(t) - P\left(t - \tau / t_{\min}\right) \tag{2}$$

where t_{min} = 5 minutes for the BPA case.

Next, the histograms for τ = 5, 10, 30, 45 and 60-minute wind variability are obtained and are shown in Figure 6. These histograms also convey the probabilistic interpretation of variability. Each histogram is formed using 50 by 50 grids (with different bin widths), and all those have been overlaid for ease of visual comparison. It is worth noting the increasing variance in the empirical histograms as the time intervals become longer.

III.D. Distributions Considered for Fitting the Empirical Data

Mean, μ and variance, σ^2 are the primary parameters that describe a normal distribution. Additionally, skewness and kurtosis are important descriptors of the shape of a distribution. Skewness, as defined in (3) is the measure of lack of symmetry of a distribution, and kurtosis, as defined in (4), indicates the degree of peakedness of a distribution

$$\gamma = \frac{\mu_3}{\mu_2^{3/2}} \tag{3}$$

$$\kappa = \frac{\mu_4}{\mu_2^2} \tag{4}$$

where μ_i is the i-th central moment of the distribution.

The histograms in Figure 6 are not exactly symmetric about the variability axis. Moreover, the histograms for smaller time durations are very peaky. As normal density functions cannot capture such characteristics very well, we need to consider other PDF besides normal. While the symmetric double exponential, *i.e.* the Laplace distribution, could be a potential match (to

capture the peakedness of the data), we need a more generalized model of the Laplace distribution to properly capture the asymmetry of the observations [21].

III.D.1. The Skew-Laplace Distribution

The PDF of a skew-Laplace distribution of a random variable x is described by equation (5) using the parameters μ, α and β [20], [21].

$$g(x;\alpha,\beta,\mu)=\frac{1}{\alpha+\beta}\begin{cases}\exp\left(\frac{x-\mu}{\alpha}\right), & x\le\mu\\ \exp\left(\frac{\mu-x}{\beta}\right), & x>\mu\end{cases} \tag{5}$$

The use of the α and β parameters enables the skewness in this modified form of the double exponential distribution whereas μ serves as the locational (centering) parameter. Formulae for cumulative distribution function (CDF) and maximum likelihood estimates (MLE) for the parameters of a SKL RV are available in the Appendix A.

III.E. Goodness of Fit

Besides comparing the fitted distribution with the histograms graphically, we can compare the CDFs to test the goodness of fits [20]. Once we obtain the MLE from the dataset, we can generate a CDF and visually compare it with the empirical CDF obtained using the ECDF function in MATLAB which applies the Kaplan-Meier estimate of the CDF [39].

III.F. Power Spectral Density Estimation

The PSD of aggregated wind turbine outputs provides information on the characteristic of fluctuations in the output [40], [41], [42], [43]. One method to estimate the PSD is through the computation of the periodogram [40], which we have followed in our work. One of the attributes

of the power spectrum estimation through periodograms is that increasing number of samples does not reduce the variance of the estimate. Instead a segmenting and averaging technique should be used instead. The overall dataset can be partitioned into *k* segments, while the Fourier transform of each segment is taken and a periodogram estimate is constructed for the limited-duration segment. The actual periodogram is obtained by averaging the *k* sub-PSD at each frequency. This technique (i.e. the use of a window function) helps reduce the variance of the final estimate by a factor of *k* [40]. As argued by Apt in [40], the PSD estimate of wind power provides an estimate of the average wind power variability over time intervals 1/*f*. We need to underline, however, that the PSD estimates the absolute value of the wind power variability.

In the following section, the results of the estimation techniques will be incorporated in the Unit Commitment. Primarily, the α and β parameters of the SKL distribution provide the standard deviations of the wind power variability and hence typically three standard deviations will be used to set the ramp requirements.

III.G. Modified Unit Commitment with Wind

After establishing the parameters to represent intra-hour wind behavior, here we revisit the standard unit commitment [15], [16] to incorporate the developed sub-hourly features. Since UC involves hourly scheduling, with $t = 1, 2, 3, \ldots, 24$, we want to incorporate intra-hour variability and ramp behavior inside UC. Thus, indices corresponding to intra-hour segments need to be included. In Figure 7, the indices of intra-hour segments, $\phi = 1, 2, \ldots, 6$ represent durations, $\tau_\phi = 10, 20, 30, 40, 50, 60$ minutes respectively.

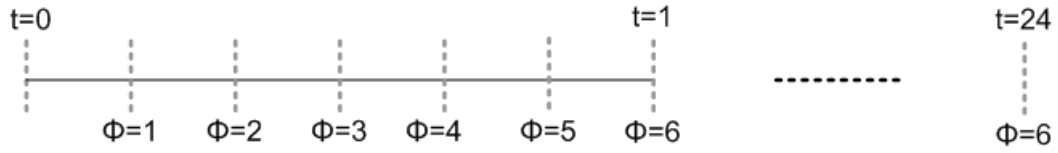

Figure 7. Hourly and sub-hourly time indices for unit commitment

III.H. Sub-hourly Wind Behavior in UC

First, assuming time-stationarity property which implies that the parameters of the wind variability PDFs are time invariant, the mean of 5-minute up-ward variability, $w_{t\phi}^{\text{var}-up-5\text{min}}$, can be used to obtain the upward variability for sub-hourly intervals in the following manner,

$$\tilde{w}_{t\phi}^{\text{var}-up} = \left(\tau_\phi / 5\right) w_{t\phi}^{\text{var}-up-5\text{min}} \tag{6}$$

Here, $w_{t\phi}^{\text{var}-up-5\text{min}}$ can be set to three standard deviations of the wind variability PDF fitted by SKL distribution using techniques detailed in the previous sections. Similarly, downward variability for sub-hourly intervals ϕ with $\tau_\phi = 10, 20, 30, 40, 50, 60$ can obtained using the 5-min downward variability, $w_{t\phi}^{\text{var}-dn-5\text{min}}$, from the following equation,

$$\tilde{w}_{t\phi}^{\text{var}-dn} = \left(\tau_\phi / 5\right) w_{t\phi}^{\text{var}-dn-5\text{min}} \tag{7}$$

Without considering time-stationarity, we can directly use the parameters obtained for variability over each time intervals, $\tilde{w}_{t\phi}^{\text{var}-up}$ and $\tilde{w}_{t\phi}^{\text{var}-dn}$. Note that we need to take into account that upward wind variability cannot exceed the installed wind capacity, therefore the parameter need to be adjusted accordingly for use in UC.

$$w_{t\phi}^{\text{var}-up} = \min\left(w_{\max} - w_t^f, \tilde{w}_{t\phi}^{\text{var}-up}\right) \tag{8}$$

Similarly, downward variability is restricted by the difference in forecasted output and the minimum,

$$w_{t\phi}^{\text{var}-up} = \min\left(w_t^f - w_{\min}, \tilde{w}_{t\phi}^{\text{var}-dn}\right) \tag{9}$$

III.I. Ramp Characteristics in UC

Given the generator upward ramp rate limit, $r_i^{up-rate}$, in MW/min, a generator is expected to ramp linearly up to $r_i^{up-rate}\tau_\phi$ MW over τ_ϕ duration during the hour. Many fast ramping generators are able to reach full capacity before the end of the hour [29]. Therefore, the ramp up capacity during the hour at intervals ϕ with $\tau_\phi = 10, 20, 30, 40, 50, 60$, can be obtained by,

$$R_{i\phi}^{up} = \min\left(g_i^{\max} - g_i^{\min}, r_i^{up-rate}\tau_\phi\right) \tag{10}$$

Similarly, the down ramp capability can be obtained from the following expressions,

$$R_{i\phi}^{dn} = \min\left(g_i^{\max} - g_i^{\min}, r_i^{dn-rate}\tau_\phi\right) \tag{11}$$

The generators must be able to provide enough sub-hourly flexible capacity to meet the sub-hourly variability in wind. Therefore, the sum of the up (down) reserve capacities up to sub-hourly interval must at least exceed the upward (downward) variability for the same interval.

$$\sum_i r_{it\phi}^{up} \geq w_{t\phi}^{\text{var}-up} \tag{12}$$

$$\sum_i r_{it\phi}^{dn} \geq w_{t\phi}^{\text{var}-dn} \tag{13}$$

Next to incorporate the sub-hourly ramp limits, we first analyze the hourly case. In a UC with hourly time resolution generation and up reserve is limited by hourly constraints detailed in Appendix B.

Figure 8 illustrates the hourly availabilities of ramp capacities of a generator. For example, the generator with capacity, $g_i^{\max}$ = 100 MW, is set at $g_{i(t=0)}$ = 40 MW at hour t = 0 and $g_{i(t=1)}$ = 70 MW and t = 1. With hourly ramp limit of 60 MW/hour, $R_i^{up} = 60\,\text{MW}$, the generator output can reach $g_i^{\max} = 100\,\text{MW}$ at hour t=1. Therefore, it can provide upward capacity of up to $g_i^{\max} - g_{i(t=1)}$ = 30 MW. On the contrary, it can provide 70 MW of downward capacity. However, this representation does not explicitly incorporate the intra-hour behavior of the generator, which will be explained next.

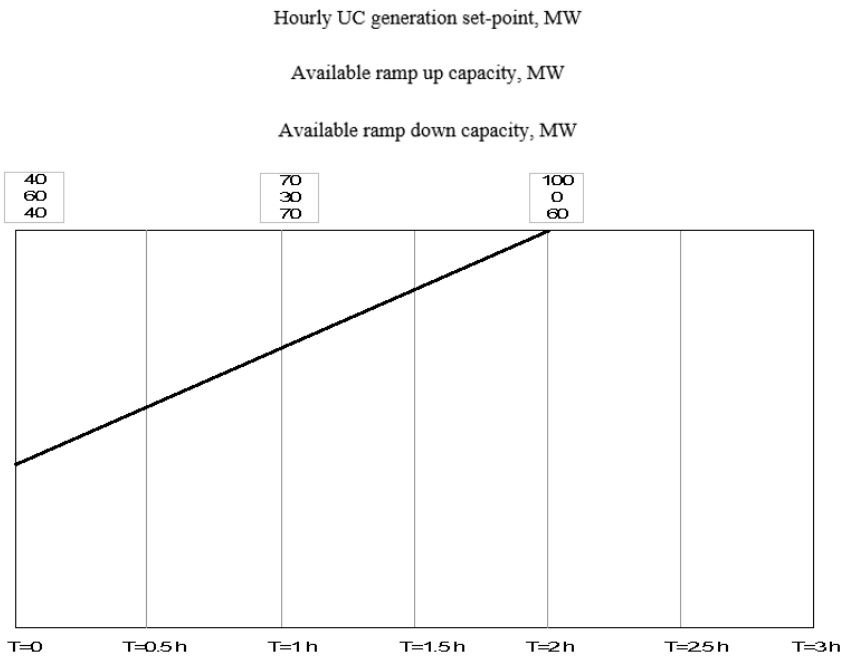

Figure 8. Hourly generation levels with up and downward capabilities

For comparison, in Figure 9, the sub-hourly behavior is shown. Here, we assume a linear ramping process for the generator (ramp rate 1 MW/min or equivalently 60 MW/h). Besides the hourly output levels, the output levels are shown also at every 30-min intervals. While generation commitment decisions are taken only at hourly intervals, the sub-hourly output levels, $g_{it\phi}^{s}$, are

needed at different intra-hour durations so that the intra-hour upward and downward capabilities can be computed.

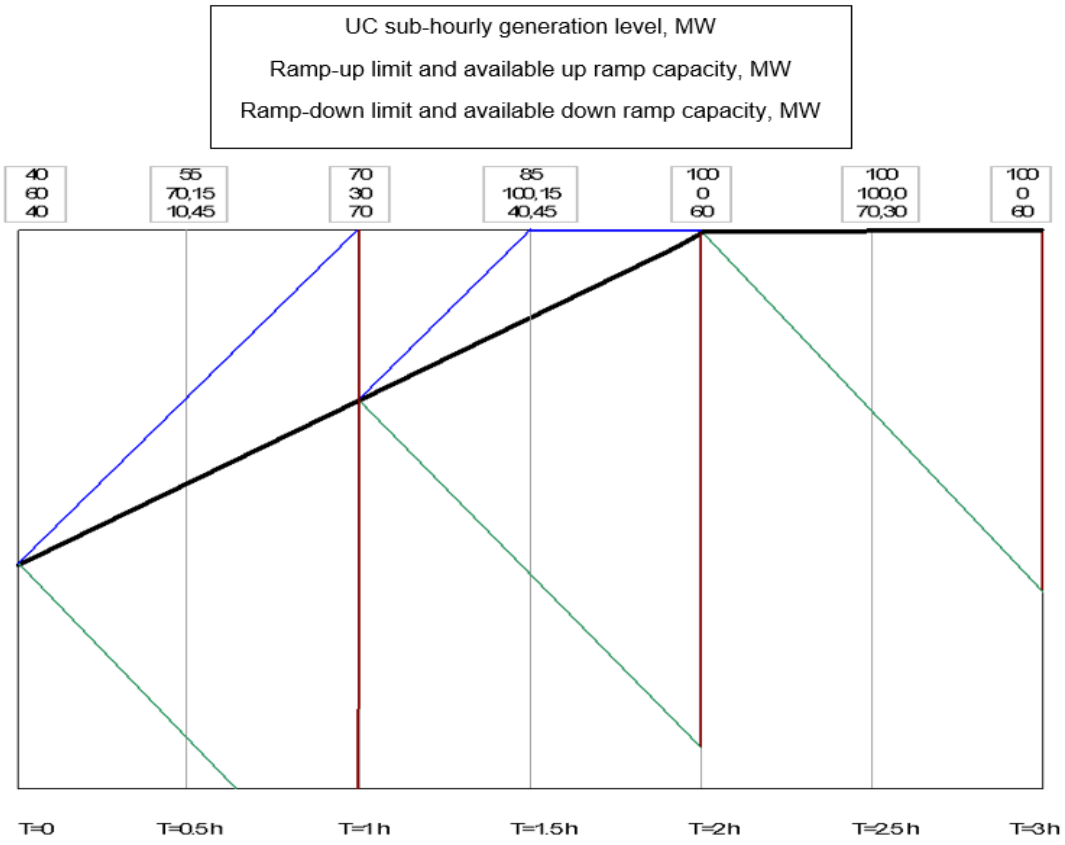

Figure 9. Sub-hourly generation levels with up and downward ramp limits and available flexible ramp capacities

At $\tau_\phi = 60$ minutes, $g^s_{it\phi}$ must be equal to g_{it}. Moreover, since a generator ramps at the rate, $\frac{g_{i(t+1)} - g_{it}}{60}$ MW/min, at τ_ϕ minutes, it must be $\left(\frac{g_{i(t+1)} - g_{it}}{60}\right)\tau_\phi$ higher (or lower if this quantity is negative) than $g_{i(t-1)}$. Therefore,

$$g^{s}_{it\phi} = g_{i(t-1)} + \left(\frac{g_{it} - g_{i(t-1)}}{60} \right) \tau_{\phi} \tag{14}$$

Next, we let $R^{up}_{i\phi}$ be the up ramp limit of generator *i* for sub-hourly interval ϕ with duration τ_{ϕ}. Then, the generators total output at duration τ_{ϕ} must be limited by $g_{i(t-1)} + R^{up}_{i\phi}$ when ramping up and by $g_{i(t-1)} - R^{dn}_{i\phi}$ when ramping down. Therefore, the combined sub-hourly generation, $g^{s}_{i(t-1)\phi}$, and upward reserve, $r^{up}_{i(t-1)\phi}$, must respect (15).

$$g^{s}_{i(t-1)\phi} + r^{up}_{i(t-1)\phi} \leq g_{i(t-1)} + R^{up}_{i\phi} \tag{15}$$

Similarly, the sub-hourly generation levels, $g^{s}_{i(t-1)\phi}$, less the downward reserve, $r^{up}_{i(t-1)\phi}$, must respect (15).

$$g^{s}_{i(t-1)\phi} - r^{dn}_{i(t-1)\phi} \geq g_{i(t-1)} - R^{dn}_{i\phi} \tag{16}$$

Finally to ensure that the generation maximum and minimum capacity limits are not violated at any time, we must also include constraints (17) and (18).

$$g^{s}_{i(t-1)\phi} + r^{up}_{i(t-1)\phi} \leq g^{\max}_{i} u_{it} \tag{17}$$

$$g^{s}_{i(t-1)\phi} - r^{dn}_{i(t-1)\phi} \geq g_{i(t-1)} u_{i(t-1)} \tag{18}$$

As seen from Figure 9, if a generator is already in an upward ramp trajectory due to an hourly set point change then up reserve potential during the sub-hourly interval reduces, while the down ramp potential increases.

Overall, the following constraints have been added to the standard formation presented in Appendix B.

$$g^{s}_{it\phi} = g_{i(t-1)} + \left(\frac{g_{it} - g_{i(t-1)}}{60} \right) \tau_{\phi}$$

$$\sum_{i} r^{up}_{it\phi} \geq w^{\text{var}-up}_{t\phi}$$

$$\sum_{i} r^{dn}_{it\phi} \geq w^{\text{var}-dn}_{t\phi}$$

$$g^{s}_{i(t-1)\phi} + r^{up}_{i(t-1)\phi} \leq g_{i(t-1)} + R^{up}_{i\phi}$$

$$g^{s}_{i(t-1)\phi} - r^{dn}_{i(t-1)\phi} \geq g_{i(t-1)} - R^{dn}_{i\phi}$$

$$g^{s}_{i(t-1)\phi} + r^{up}_{i(t-1)\phi} \leq g^{\max}_{i} u_{it}$$

$$g^{s}_{i(t-1)\phi} - r^{dn}_{i(t-1)\phi} \geq g_{i(t-1)} u_{i(t-1)}$$

In the next Chapter, first we present the results related to sub-hourly characterization of wind behavior. Next, these results will be incorporated into the UC model. Finally, several Unit Commitment case studies will be presented to analyze the impacts on power systems operations and planning.

Chapter IV Results and Analyses

IV.A. Analysis in the Time Domain

The time series of the 5-minute variability of the BPA wind data is shown in Figure 10. The Mean of positive changes was at 0.0059 p.u. and the mean of negative changes was at -.0055 p.u. The standard deviation of positive changes was at 0.0070 in p.u. and the standard deviation of negative changes was at 0.0063 pu.

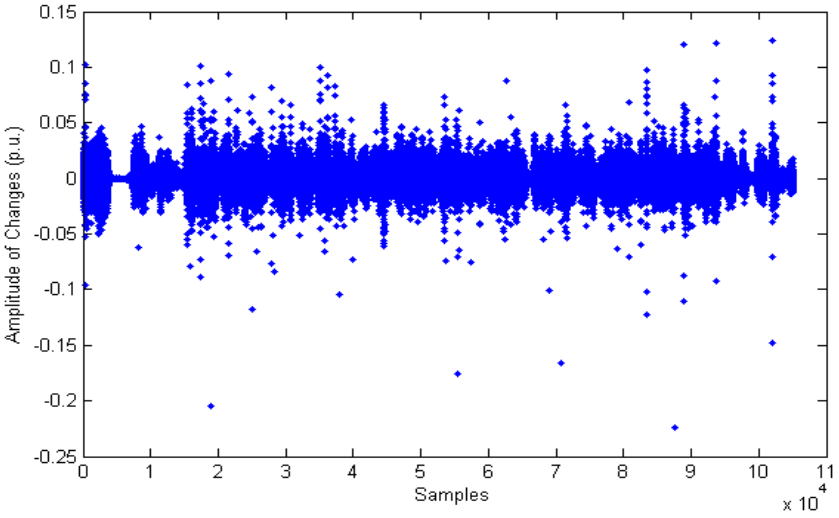

Figure 10. Time series of 5 minute variability

IV.A.1. Generation Level Dependency of Variability:

The mean generation level was at 0.2873 p.u. Next, we partitioned the 5-minute wind variability data based on the generation levels, i.e. the variability observed when wind level was above and below mean. These 5-minute changes are defined as Δ^{w_high} and Δ^{w_low}. These changes

are plotted in Figure 11. Similarly, 60-min changes, conditioned on generation levels, were obtained. Table II presents the mean and standard deviation of these 5-min and 60-min changes.

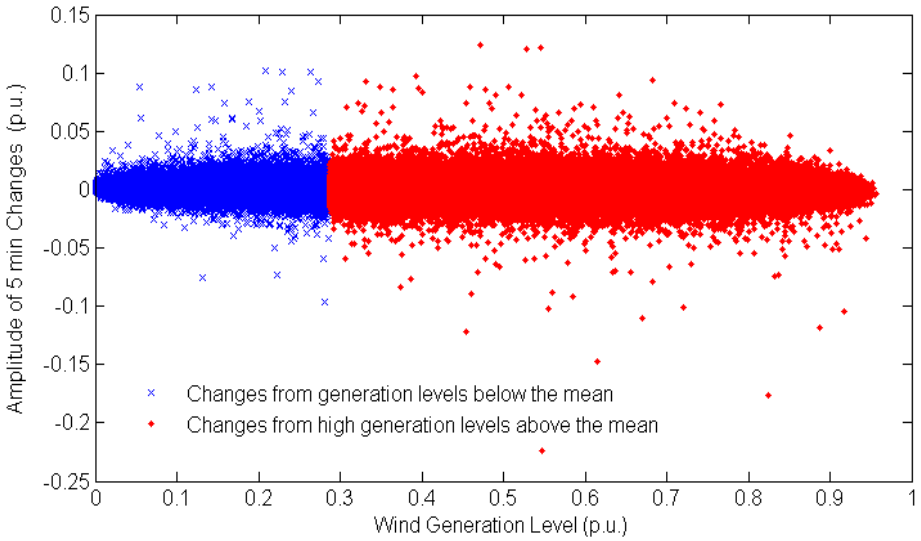

Figure 11. Generation level versus 5 min changes

Table II Mean and standard deviation of changes based on generation levels

Intervals	Mean Δ^{w_low} (p.u.)	Std Δ^{w_low} (p.u.)	Mean Δ^{w_high} (p.u.)	Std Δ^{w_high} (p.u.)
5-min	0.0001	0.0052	-0.0001	0.0114
60-min	0.0039	0.0424	-0.0060	0.0753

As shown in Table II, the mean of changes from 'high' generation levels have a downward tendency (stronger for the 60 minute case) whereas the mean of changes from 'low' states have an upward tendency. This matches our intuition that when wind power output is already at a high level, the room for upward changes is much smaller than what it could be when the output level is low. Moreover, for changes from high levels, variability can be described using a normal

distribution which is due to the fact that when wind output levels are high, the 60 minute fluctuations have less probability of being distributed only tightly around the mean. But for other cases, especially for short duration intra hour variations, these are tightly centered around the mean. Thus, we need to analyze the performance of Laplace distributions compared to normal for those.

IV.A.2. Time Duration Dependency of Variability:

Table I shows the maximum positive and negative changes (in p.u.) for time durations, τ = 5, 10, 30, 45 and 60 minutes. For τ = 5 and 10 minutes negative changes (down ramps) were larger whereas in the other cases positive changes were larger. Also, the kurtosis, which captures the peakedness, is highest for 5 minute intervals and as time duration increases, kurtosis decreases.

Table III Maximum Positive and Negative Changes

Time Duration (minutes)	(–) Δ	(+) Δ	Kurtosis
5	–0.2237	0.1238	29.89
10	–0.2369	0.2086	18.69
30	–0.2727	0.3955	10.99
45	–0.3525	0.4627	9.66
60	–0.4152	0.5354	8.91

As shown in the previous section, wind distribution parameters vary for low and high wind. Since with larger time intervals, wind has higher possibility to change regime and move from a low to a high state or vice versa, the wind distribution parameters must also be dependent of time intervals.

Table IV Best Fit Parameters

Time Duration (minutes)		Normal		Skew-Laplace	
	μ	σ	μ	α	β
5	0	0.008	0	0.0050	0.0050
10	0	0.0144	0	0.0087	0.0087
30	0	0.0345	0	0.0214	0.0213
45	0	0.0469	0	0.0293	0.0292
60	0	0.0579	0	0.0364	0.0363

In Figure 12-Figure 15, we present the empirical histograms of normalized wind power variability for time duration, τ = 5, 10, 30, and 60 minutes. The dotted lines overlaid on top of the histograms represent the skew-Laplace (SKL) best fits whereas the dashed lines represent the normal distribution fits. The maximum likelihood estimates (MLEs) for the parameters of normal and SKL are shown in Table IV.

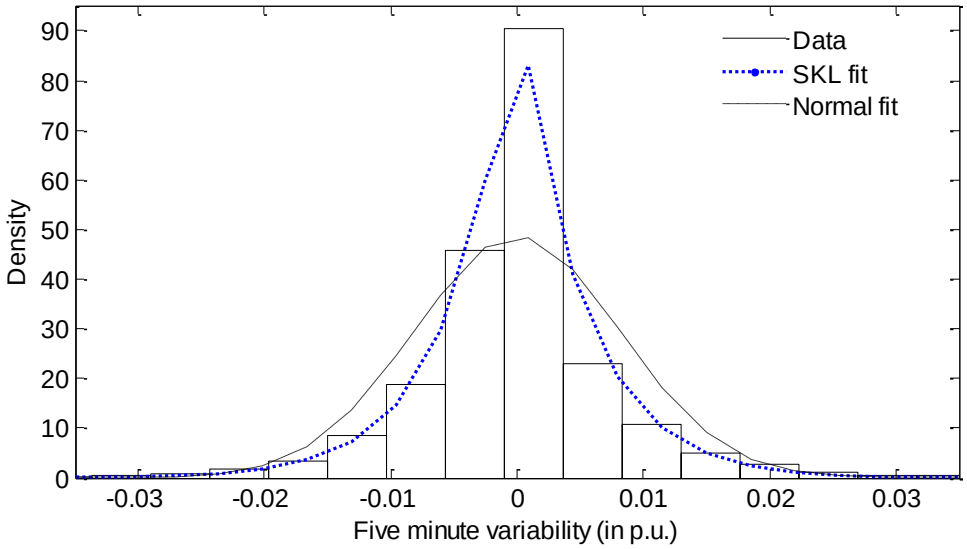

Figure 12. Curve fitting (PDF) for 5 minute variability

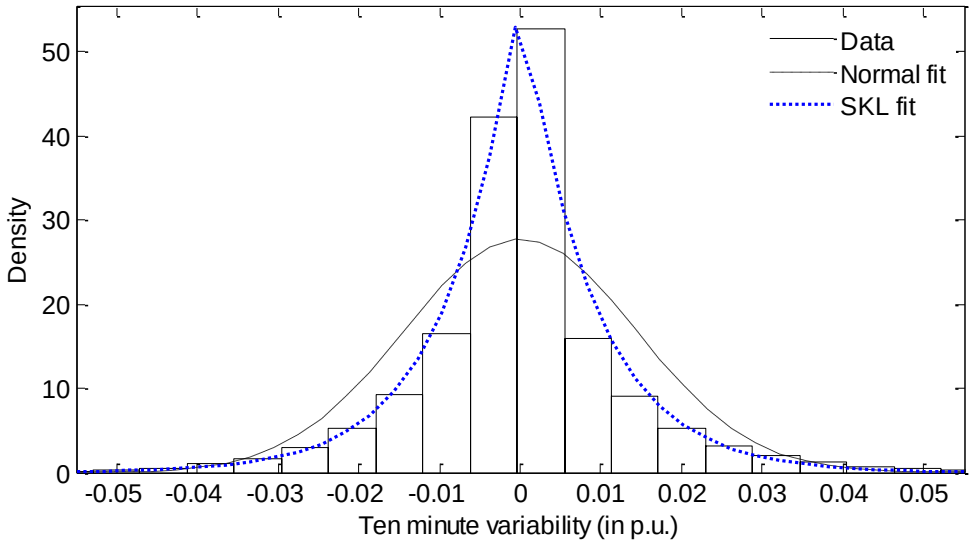

Figure 13. Curve fitting (PDF) for 10 minute variability

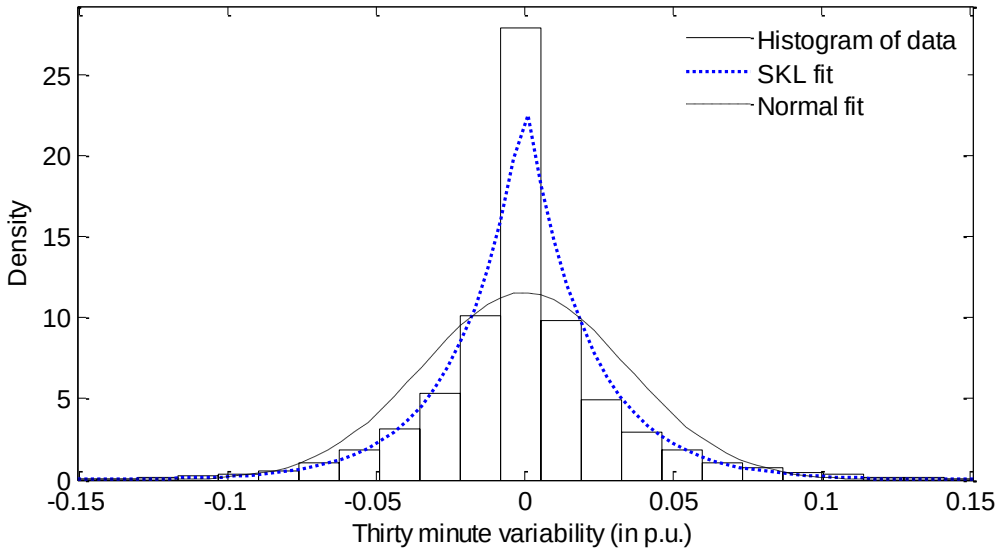

Figure 14. Curve fitting (PDF) for 30 minute variability

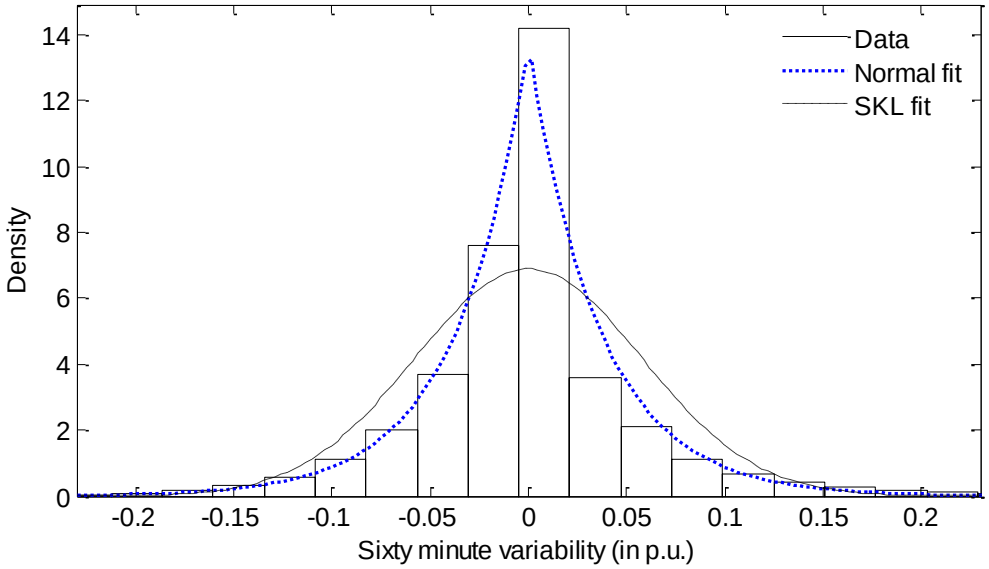

Figure 15. Curve fitting (PDF) for 60 minute variability

IV.A.3. Goodness of Fit:

To test the goodness of the various fits, we compare the theoretical and empirical cumulative distribution functions (CDFs). In Figure 16, the solid lines represent the empirical CDFs, the

dotted lines the SKL and the dashed lines the normally-distributed fits with estimated best fit parameters computed from the data samples.

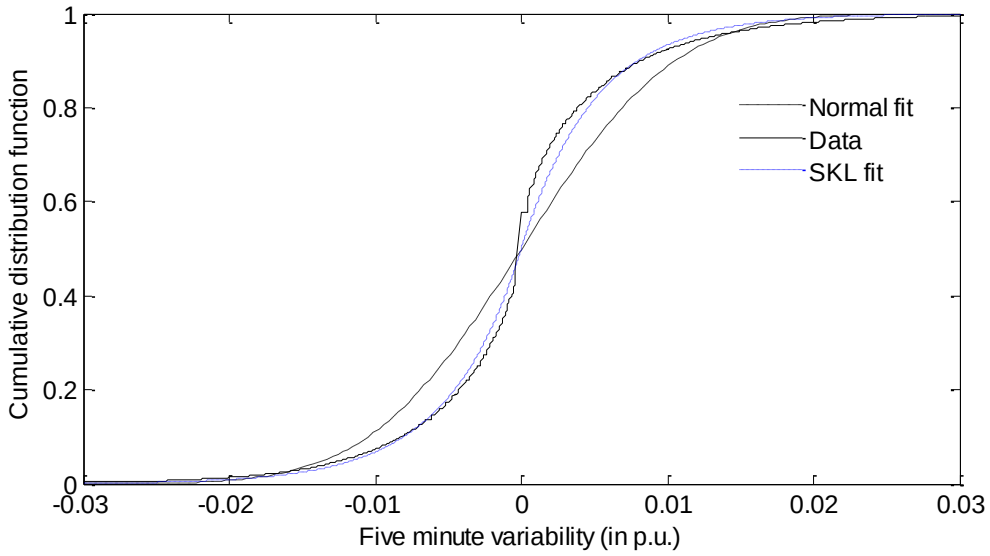

Figure 16. Goodness of fit test for 5 minute variability

Only the plots for the 5-minute variations are shown since the other cases show similar characteristics. The plot confirms that the normal fits are not appropriate to the empirical distribution, whereas SKL follows the empirical distribution much more closely.

IV.A.4. Additional Conditional Aspects

Generally, nighttime (7 pm to 7 am) wind variability data showed higher positive skewness than during daytime (7 am to 7 pm). While daytime 5-minute variations had skewness of (-0.39), the night time data had a skewness of 0.16. More specifically, for May-August, the night time 60 minute variability data had a skewness of 1.43, which was higher than the daytime skewness of 0.29. Thus we observed that the summer night data had a relatively high positive skewness. In Figure 17, the dashed line represents a symmetric Laplace fit whereas the solid line represents a

SKL fit. It clearly demonstrates the benefit of using SKL over Laplace when the histogram lacks symmetry about the distribution peak.

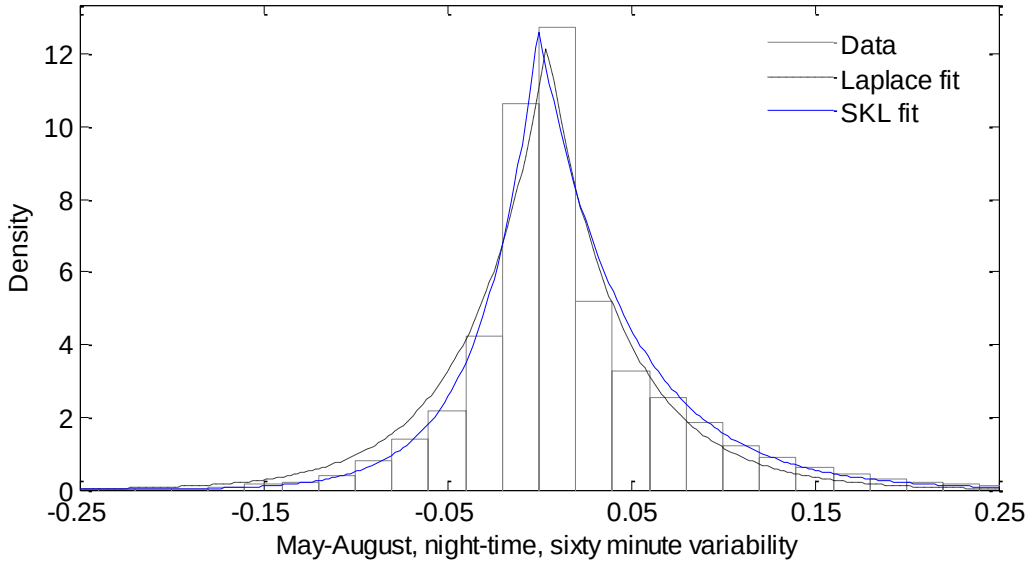

Figure 17. Curve fitting for May-August, nighttime, 60 minute variability

IV.B. Analysis in the Frequency Domain

Figure 18 presents the PSD estimate of the BPA 2009 wind output data. The Nyquist frequency here is 1.68×10^{-3} Hz for the data with resolution of 5 minutes. To reduce variance of the estimate, eight segments were used. The frequency range is from 2.54×10^{-7} Hz to 1.68×10^{-3} Hz (1 Hz = 1 s^{-1}). We can notice a peak at approximately 1.2×10^{-5} Hz which indicates the presence of a daily cycle driving the variability of wind power.

As seen in Figure 19, the linear region of the power spectrum plot (in log-log scale) indicates that the PSD fits an exponential function of frequency (proportional to $f^{-2.4}$, *i.e.* as the slope of the periodogram is –2.4). To obtain this best fit, we used a robust fitting in MATLAB where by

default the algorithm uses iteratively a reweighted least squares with bi-square weighting functions [39].

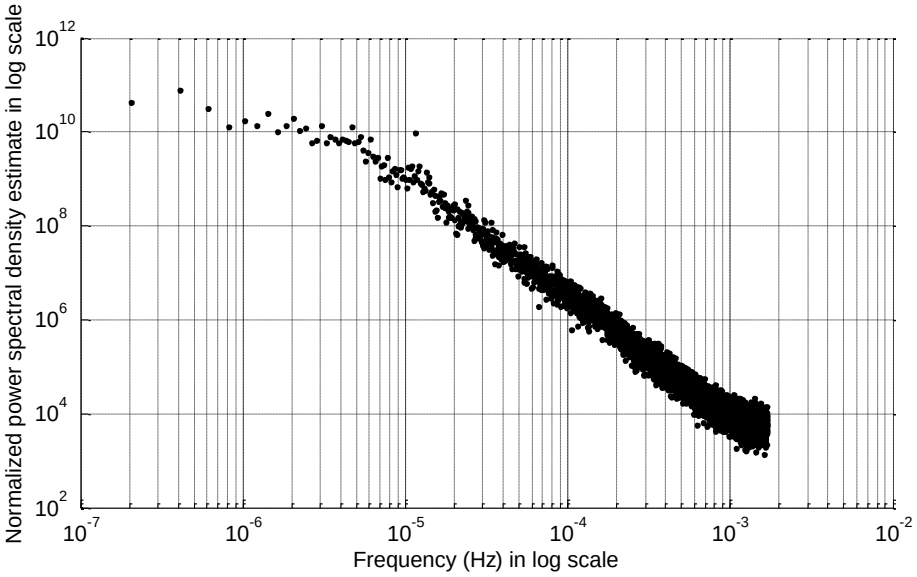

Figure 18. Power spectrum of aggregate wind data from the BPA control area sampled at 5 min resolution from January 1, 2009 to December 31, 2009.

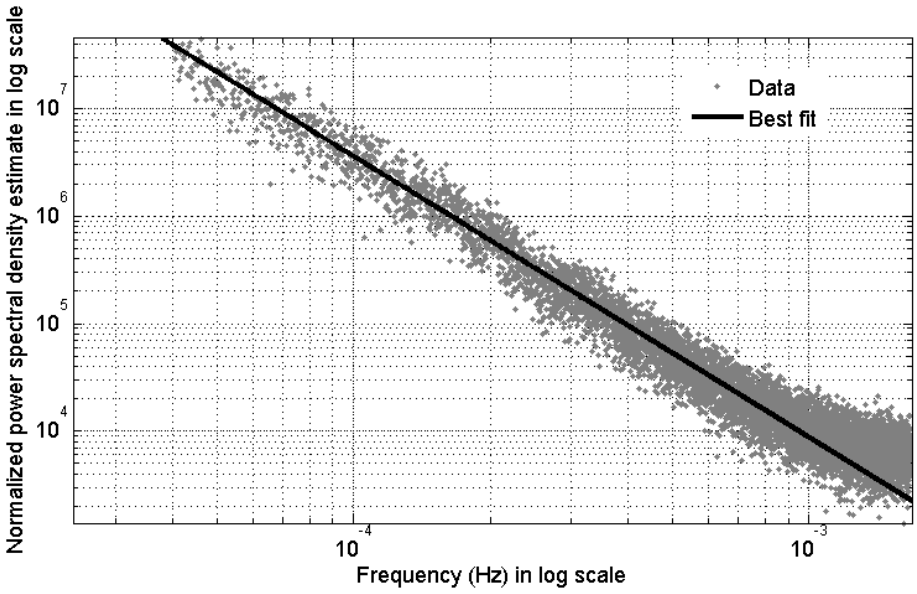

Figure 19. Linear region of the PSD fitted by an exponential function of the frequency

Since the PSD follows a fairly predictable shape even though wind behavior is random, the availability of best fit parameters for the PSD can be used to improve forecasting techniques. Moreover, it could be useful to generate stochastic profiles for different intervals of wind which will respect the PSD of the true random process.

One approach to generate the synthetic profiles is by forming a Markov chain representation of wind power (or wind speed) [45]. The output levels can be discretized and a state transition matrix can be formed to describe how the outputs change given the current and past states. In a first-order Markov process the future states can be predicted only from the current state and is thus independent of any past states, whereas, an n-th order Markov model would require the current as well as $(n - 1)$ past states. The Markovian representation is appealing since it incorporates temporal correlation unlike the simplistic Monte Carlo-based approaches and therefore have been examined by several studies [45]-[48]. In [46], authors use a first order model with an 8 by 8 transition matrix for hourly time step and they state that higher order models will be investigated in their future work for a more accurate representation. Authors in [48] provide a formal proof that a first order Markov will be able to reproduce the correct probability distribution function, however, the matching of the autocorrelation will depend on the number of states, the order of the chain and the time step being considered. The lack of matching of the autocorrelation was also observed in the first and second order models presented in [47]. Therefore the generation of synthetic profiles must consider the autocorrelation or the PSD as an important model validation measure when considering Markovian representations.

IV.C. Unit Commitment Case Studies

IV.C.1. Generator data

We consider a three-generator power system with a total generation capacity of 250 MW. Table V defines the generator capacities (Max/Min), incremental costs (IC), shutdown and start-up costs (SDC/SUC), incremental costs of providing ramping (RIC), and minimum up and down times (MUT/MDT).

Generators produce power at constant incremental costs in $/MWh with negligible fixed costs. Reserve incremental costs apply to generator-supplied spinning reserve scheduled to respond to potential imbalances. Ramp limits are set to 60%, 60% and 100% of the generators' capacities, G1, G2, G3, respectively. Generator 3 (G3) represents a flexible fast-ramping generator, whereas, G2 is mid-merit and G1 is baseload with longer minimum up and down time than the other two generators.

Table V Generator Data

	Max/Min (MW)	IC ($/MWh)	SUC/SDC ($)	RIC ($/MWh)	MUT/MDT (h)
G1	100/0	30	200	10	6/6
G2	100/0	50	200	5	2/2
G3	50/0	90	100	5	2/2

IV.C.2. Wind and Demand data

Figure 20 shows the hourly forecasts of demand and wind power over 24 hours. The demand peaks at 330 MW (at 8 am), whereas the wind peaks around 190 MW (at 11 am). Note that

during the night (0h - 6h) the high availability of wind power can supply over 60% of the hourly demand. However, here wind power dies down in the evening and reaches 115 MW. While the high penetration of wind can supply a significant portion of the demand, we are interested to analyze the impact on the rest of the generators that need to supply the residual demand as well as to supply reserve to balance imbalances caused by wind variations during operations.

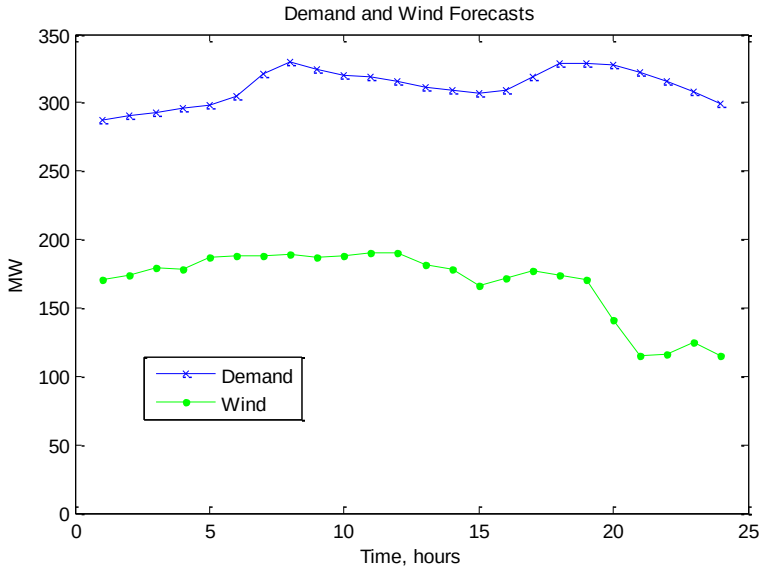

Figure 20. Demand and wind profile

IV.C.3. Results

The UC formulation developed in this thesis was programmed as a mixed integer linear program in GAMS software environment and solved via CPLEX. Results were analyzed by MATLAB.

The output of generator-1 (G1) is shown in Figure 21, for every 10 minute interval. The up and downward ramp limits for every 10-minute interval are also shown. The UC solution turns the generator on for all hours due to G1 being the cheapest generator. The generator's downward capability is limited by its ramp down limit away from the hourly generation set-points. The

generator can provide limited upward capability since it is already operating near its maximum capacity. Figure 22 shows the downward ramp capacity set for G1 by the UC to contribute to meeting the wind variability mitigation requirements, as per (13).

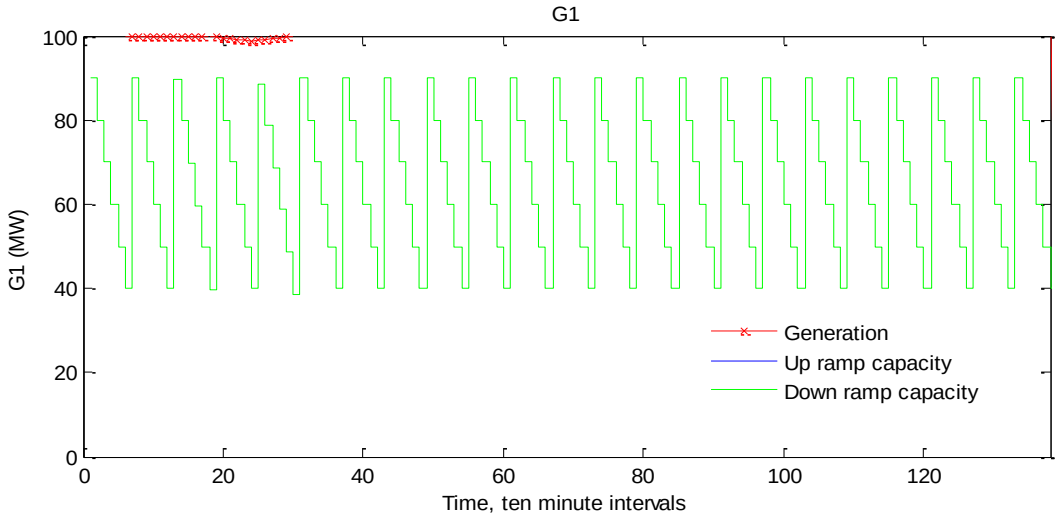

Figure 21. G1 generation and sub-hourly available capacity for up and down ramping

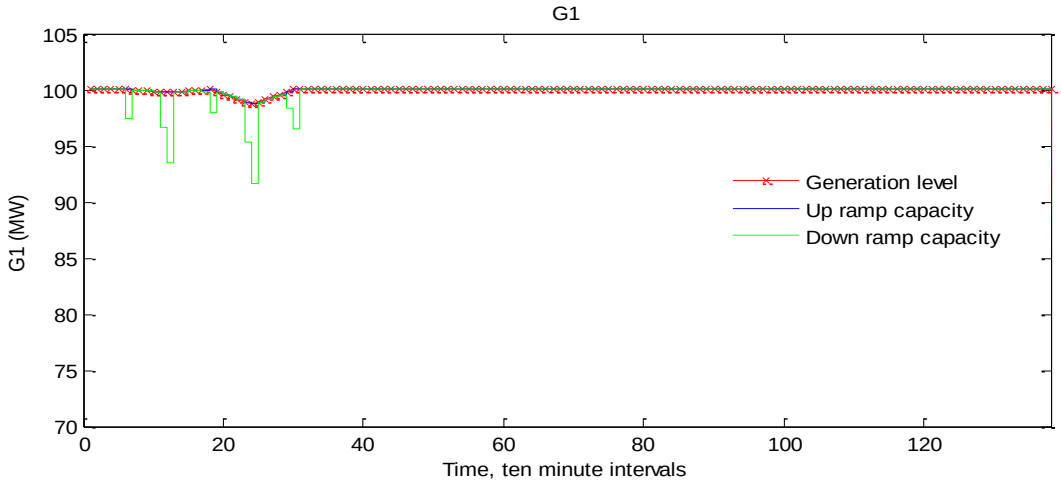

Figure 22. G1 generation and scheduled up and down ramp capacity

The output of the generator-2 (G2) is shown in Figure 23. The UC also turns the generator on for all hours. The generator, being mid-merit, balances the net demand minus the wind power

generation. Therefore, later in the evening when the wind dies down, generator-2 (G2) ramps up to full capacity to make up for the reduced output from wind.

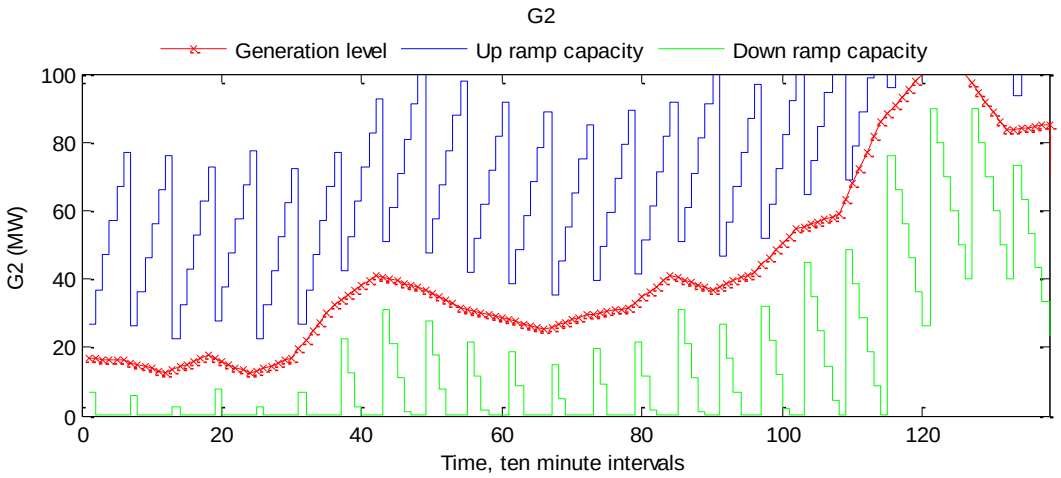

Figure 23. G2 generation and sub-hourly available capacity for up and down ramping

Generator-2's intra-hour scheduled ramp capacity, set by the UC, is shown in Figure 24. Except in the first hour, the UC prefers to ask only for down ramp capacity from G2.

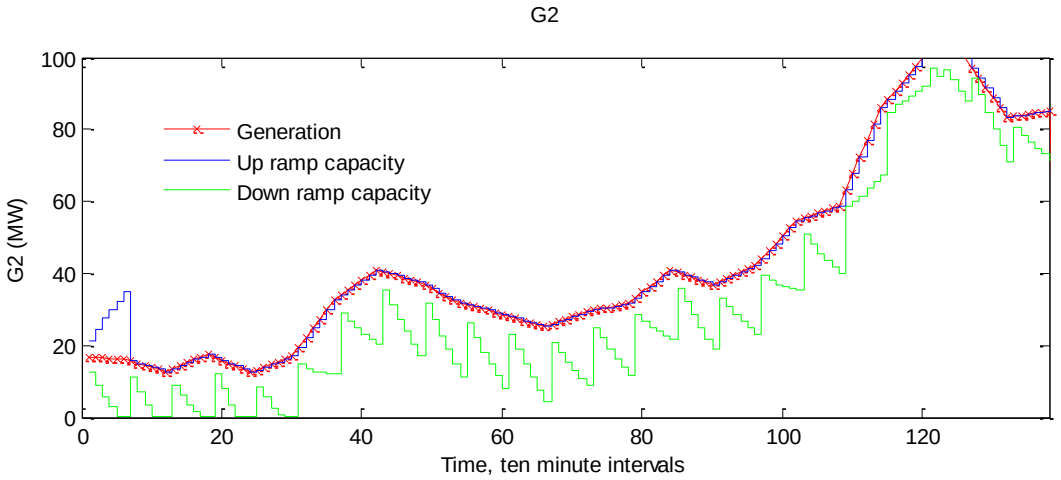

Figure 24. G2 generation and scheduled up and down ramp capacity

The output of the generator-3 (G3) is shown in Figure 25. The UC also turns the generator on for all hours, however, mostly at zero generation output. The generator upward ramp capacity is required by the UC to cover the wind variability ramping requirement (12). G3's generation and ramp capacity scheduled by the UC are shown in Figure 26.

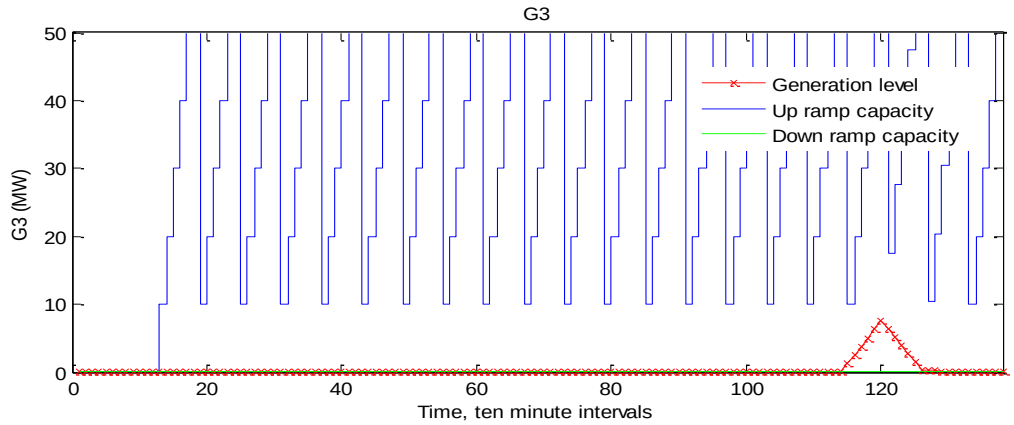

Figure 25. G3 generation and sub-hourly available capacity for up and down ramping

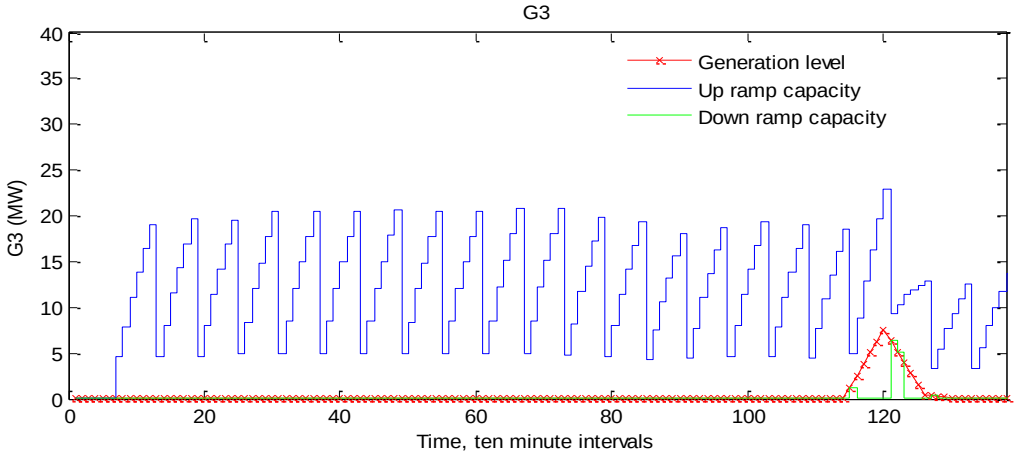

Figure 26. G3 generation and scheduled up and down ramp capacity

The aggregate available upward and downward ramp capacity limits from the generators is shown in Figure 27 and Figure 28. Due to the generators operating close to their limit, the upward capacity is lower compared to their downward ramping capacity.

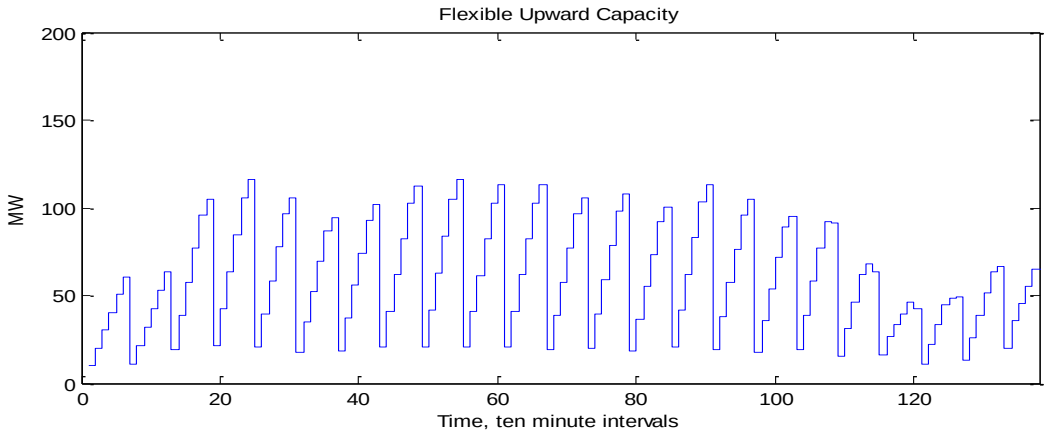

Figure 27. Aggregate available intra-hour up ramp capacity

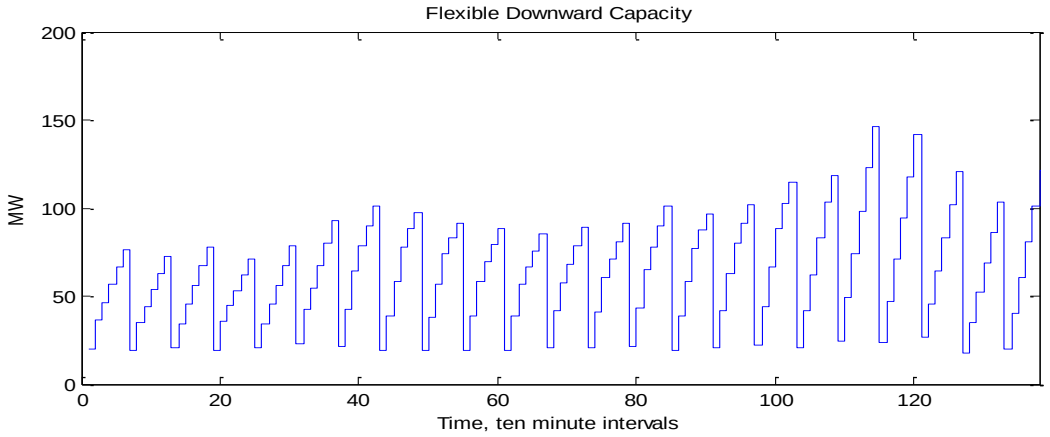

Figure 28. Aggregate available intra-hour down ramp capacity

IV.C.4. Unit Commitment Case 2

In this case, we analyze the impact of higher penetration of wind. For the same wind profile shown in Case 1, now we take a demand profile scaled down to peak at 250 MW. In this case, wind has the potential to meet 83% of the demand at hour 5. This resembles systems in Ireland, Spain and Denmark where significant wind may act as the primary energy source at several hours of the day. As we can imagine, while renewable generation is high, the baseload plants can only

generate at limited output, while the significant amount of wind might require a lot of stand by reserve from thermal generators.

The output of the generator-1 is shown in Figure 29. We see that the generator ramps up to full capacity in late evening when the wind dies down. Figure 30 shows the scheduled outputs from G2. In this case, it was not required to have G3 online.

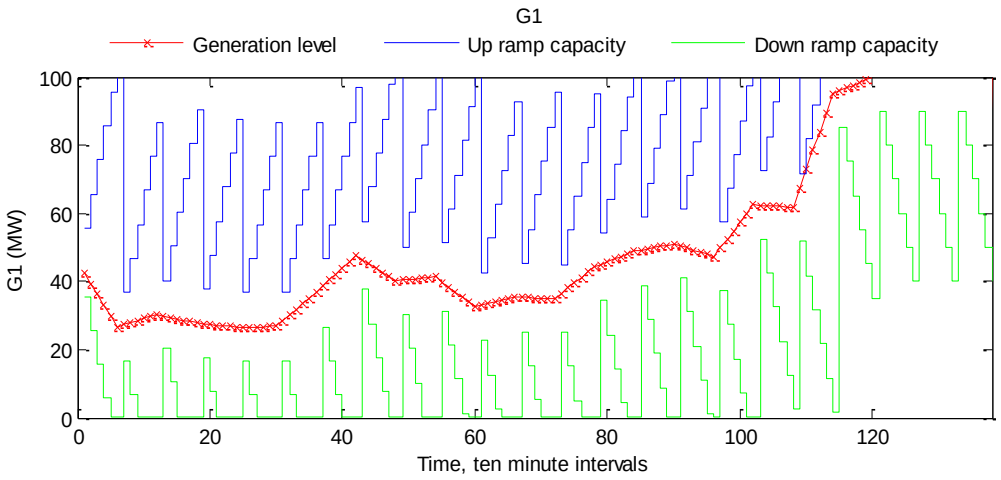

Figure 29. G1 output and sub-hourly available capacity for up and down ramping

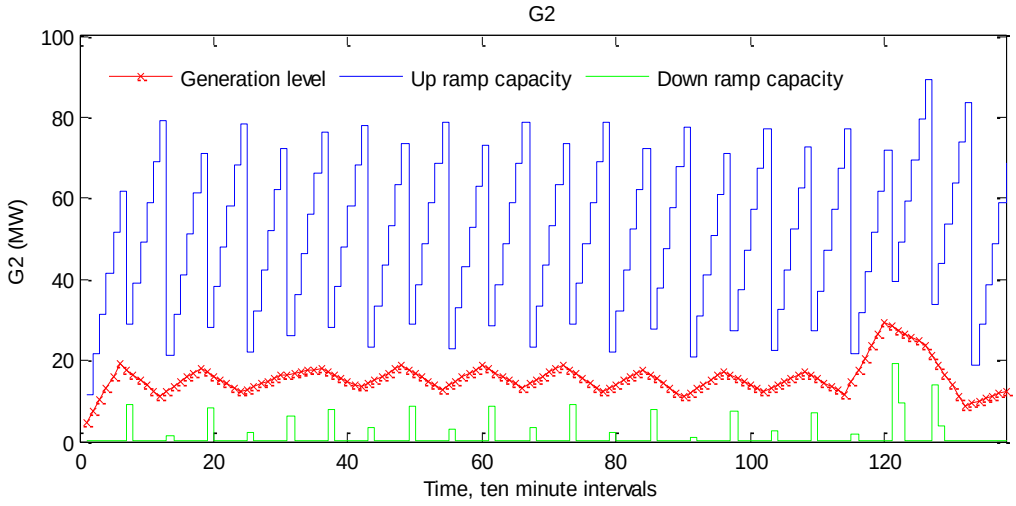

Figure 30. G2 output and sub-hourly available capacity for up and down ramping

The aggregate available up and down sub-hourly capacities can be obtained as before. Notice that in this case the upward flexibility is higher since generators are generating at a lower operating level than in Case 1 where the demand was higher.

IV.C.5. Comparison of Sub-hourly Offer Curves with the Hourly Case

In this section, we compare the behavior in the above case study (with 250 MW peak demand) with the standard Unit Commitment where only hourly reserve requirements are imposed.

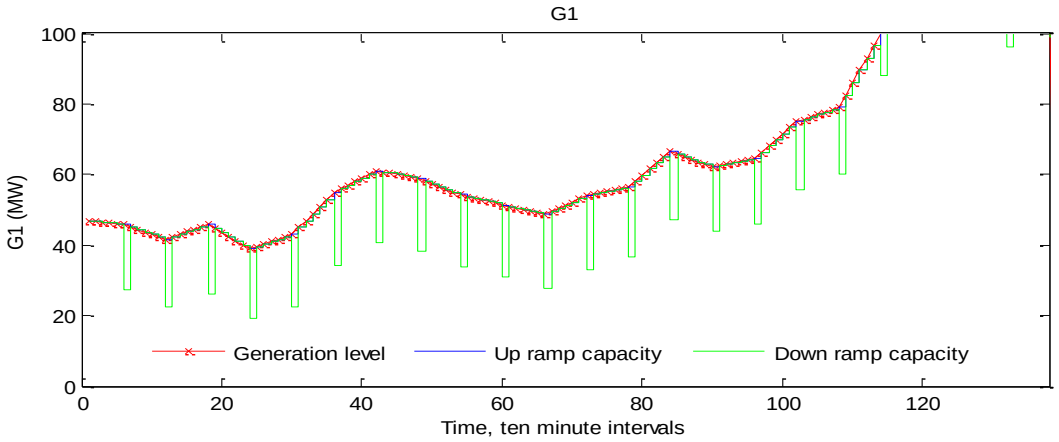

Figure 31. G1 generation and hourly scheduled capacity for up and down ramping

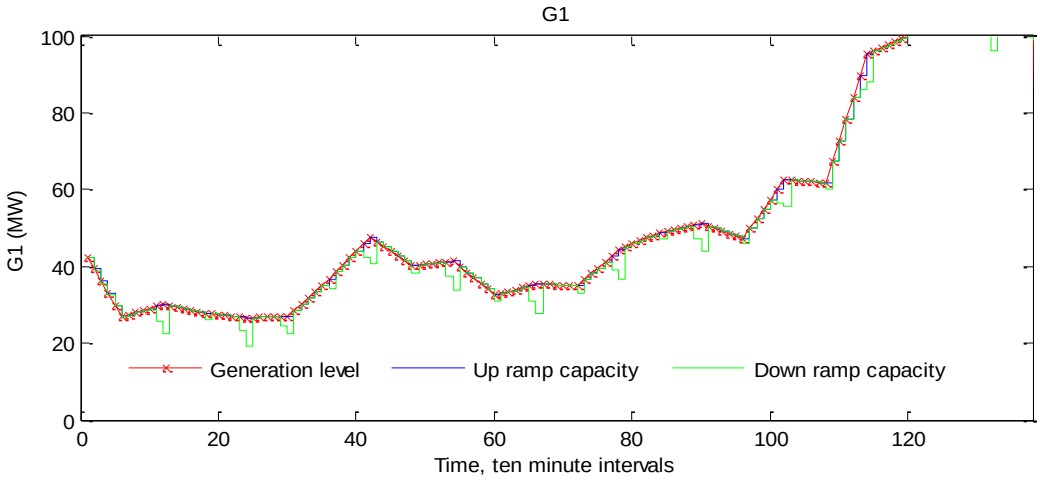

Figure 32. G1 output and sub-hourly scheduled capacity for up and down ramping

Figure 31 shows the behavior of the G1's ramping offers, where it is set by the UC to provide down ramp capability. The UC does not impose any intra-hour capacity constraints. We compare this with Figure 32, which shows the capacities set by UC by taking into account the proposed intra-hour constraints. Similarly, Figure 33 and Figure 34 show the behavior of G2's scheduled ramping capacity, without and with intra-hour constraints.

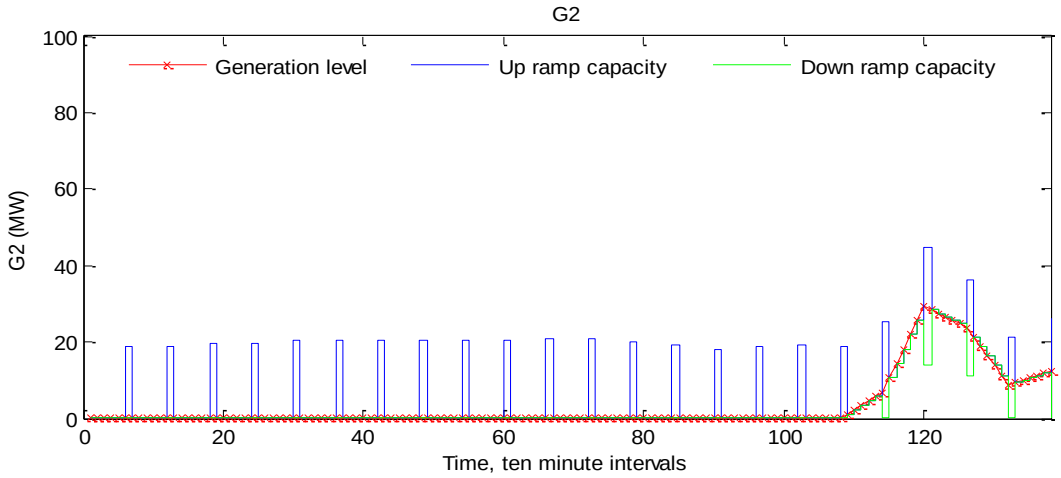

Figure 33. G2 generation and hourly scheduled capacity for up and down ramping

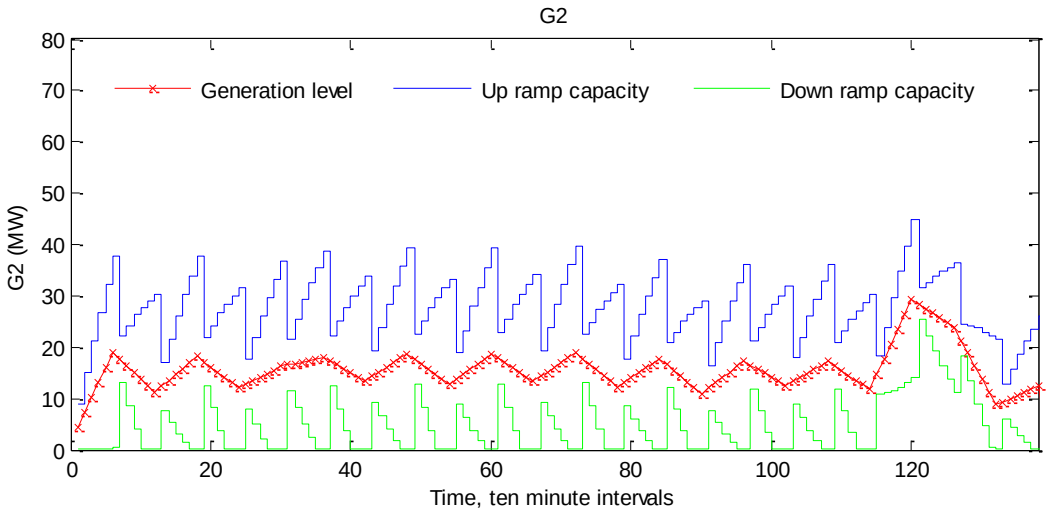

Figure 34. G2 output and sub-hourly scheduled capacity for up and down ramping

We see that, with intra-hour constraints, G2 does not operate at zero output, but rather at around 20 MW, so that it can provide both up and down ramp capability. Since G2 has lower incremental cost of ramping, it is preferable for to obtain ramping from G2, but at certain intra-hour segments, as found optimal, the UC requests for some ramp capability from G1 (Figure 32). This is not possible in the hourly case (Figure 31) due to not considering the intra-hour constraints inside the UC.

IV.C.6. Unit Commitment Case 3

Next, we simulate 30 different wind and demand profiles, as shown in Figure 35. The wind profiles randomly generated and are within two standard deviations of the original profile considered in the previous cases, whereas the demand is within 1% of the original. With these profiles, the expected day-ahead UC cost is at 56100 $/day and the expected wind curtailment is 6.9 MW (mostly at hours 3-6 and 14-16) with a maximum of 29.7 MW. Here, we required to cover three standard deviation of the wind variability. With two standard deviations, the expected day-ahead UC cost is at 49090 $/day, with almost identical curtailment.

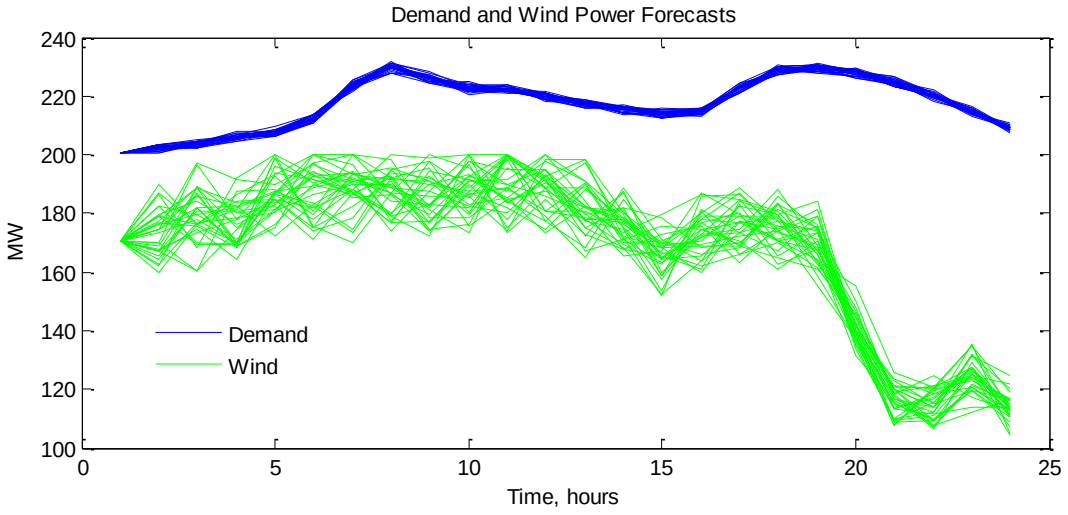

Figure 35. Test on 30 profiles of demand and wind

Another set of wind profiles were simulated and we obtained an expected cost of 87010 $/day when ramp requirements were set to cover three standard deviations of wind variability and 82460 $/day when set for two standard deviations.

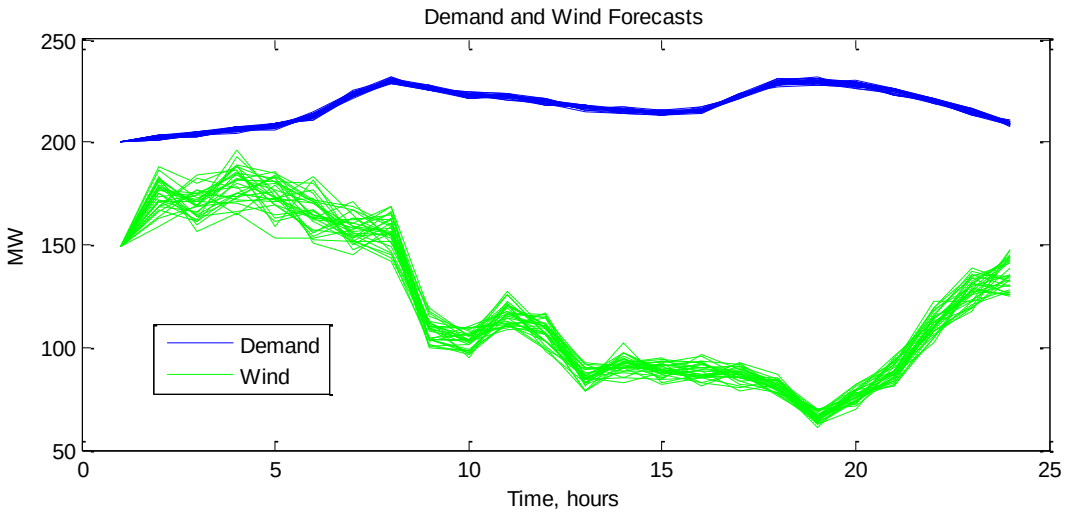

Figure 36. Test on 30 profiles of demand and wind

IV.C.7. Discussions

In the case studies, we have demonstrated that enforcing the sub-hourly constraints have an important impact on the UC results. It provides access to flexible up and down ramp capacities and the UC can utilize these capacities in the most economical way. In section IV.C.5. we noticed that the UC without considering sub-hourly constraints could not schedule generators to provide ramp capacities for only fractional intra-hour segments, which was possible through our modified UC formulation.

In Figure 34, we noticed that the output of G2 oscillates at every approximately 2-hour intervals. Since this may seem undesirable, with further investigation, we found that since G1 and G2 are the online generators, among which G2 is mid-merit, and also since G2 offers a lower incremental cost for ramp capacity, the UC utilizes G2 to provide most of the ramp capacity. To

be able to avoid the turning on of G3 while meeting the total ramp requirements for the system, UC finds it economical to allow minor oscillations in the output of G2 while it meets the ramp requirements.

Finally, in section IV.C.6. we also compared the performance of our model with stochastic profiles of wind and demand while considering different standard deviations of the wind power variability in section. We also tested on two different sets of wind profiles. When the ramp requirements were increased from two standard deviations to three standard deviations of the wind variability, we noted that the day-ahead cost increased by 14% in the first case and 5.5% in the second case, which is due to the fact that in the first case the amount of wind was much higher than the second one. Furthermore note that, even with increase in ramp requirements, in both cases there was no noticeable increase in wind curtailment which indicates there is adequate ramping capacities from generators in this test system. However, the UC plays the important role of allocating those capacities in the most economical way.

Chapter V Conclusions

With increasing wind power capacity, utilities, ISOs, regulatory bodies and researchers are trying to understand the impacts of the stochastic nature of wind power on system operations. Undoubtedly, forecasting plays an increasingly important role in improving operational efficiency, as forecasting algorithms learn from more historical data, and as they integrate the aspects inherent to wind power variability [19].

While load fluctuations are generally slow and predictable, wind ramp events are fast and unexpected and need to be managed efficiently through flexible capacity offers from supporting generators [6]. As discussed in detail in this thesis, hourly planning cannot lead to adequate reserve allocation in the presence of large wind since significantly large ramp events can occur much before the end of the hour. Both time and rate of wind ramp need to be matched optimally by generators providing operating reserve or ramp capabilities so that base and mid-load units face less cycling stress.

Through an analysis of the Bonneville Power Administration (BPA) wind power output data for 2009, we have demonstrated the need for better understanding and probabilistic modeling tools for intra-hour operations under large wind power penetrations. We noticed that histograms of wind power variability for various time intervals can be skewed and warrant the use of a more generalized probability density function, the skew-Laplace distribution, to represent this skewness. It was shown that the skew-Laplace distribution is superior to Laplace and normal distributions in expressing wind power variability characteristics, especially for intra-hour time frames. Time interval dependency, seasonal dependency and wind generation level dependency

were observed for skewness in wind power variability. Moreover, since the power spectral density of wind output data contains valuable information regarding the wind power fluctuations, we analyzed the frequency spectrum of wind power and confirmed that variability increases in proportion to $(\Delta t)^{2.4}$. Since the PSD follows a fairly predictable shape even though wind behavior is random, the availability of best fit parameters for the PSD can be used to improve variability magnitude forecasting techniques. Moreover, it could allow for the generation of stochastic wind profiles for different time intervals of wind, where the PSD of the generated profiles should match the historical PSD. The analysis techniques used here, along with the findings regarding the short-term wind characteristics, can serve as fundamental building blocks in the analysis of intra-hour operations for systems with significant wind power capacity. Furthermore, since wind PDFs were shown to be conditional on generation levels and on time durations, the simplified stationary assumption commonly invoked in unit commitment literature (with hourly resolution) needs to be revisited.

In this thesis, we incorporated the explicit intra-hour wind and generation ramp constraints into the mixed integer linear formulation of the UC. Enforcing these constraints have an important impact on the UC results, since it provides access to flexible up and down ramp capacities and harnessing these capacities in the most economical way. Thus, it can ensure secure and economic operations by taking into consideration both the wind and the thermal generator behavior in the intra-hour time frame.

Extensions of this work could include a thorough analysis of the cost-benefits through economic dispatch and Monte Carlo simulations. Detailed treatment of cycling costs, given the relevant plant operational data is accessible, and the development of flexibility metrics is also of

considerable interest. How flexible generators would compete or prefer to be paid for their capabilities is also have important area of research.

With proper quantification of intra-hour wind variability, valuation of flexible capacity offers by other generators can be modeled more effectively. For a transmission system operator, it is important to know how much the power from large wind farms is fluctuating. Our systematic wind behavior characterization can be extended to analyze local wind farm output characteristics, provided that such data is available. Optimal generation scheduling considering farm specific intra-hour wind characteristics could provide significant benefit in relieving network congestions and reducing the dependence on the curtailment of free wind energy.

Appendix A The Skew-Laplace Distribution

Skew-Laplace random variables have the PDF shown in (5) while their CDF is given by

$$G(x;\alpha,\beta,\mu)=\begin{cases}\alpha\exp\left(\dfrac{x-\mu}{\alpha}\right)\left(\dfrac{1}{\alpha+\beta}\right), x\le\mu\\ \\ 1-\beta\exp\left(\dfrac{\mu-x}{\beta}\right)\left(\dfrac{1}{\alpha+\beta}\right),\ x>\mu\end{cases} \tag{19}$$

To obtain the maximum likelihood estimation of the parameters of a skew-Laplace, we follow the method described in [20]. For a formal proof, we refer the reader to [20], [21]. We define:

$$\Delta(\mu)=\frac{1}{n}\sum_{i=1}^{n}|x_i-\mu| \tag{20}$$

$$\Phi(\mu)=\sqrt{\Delta^2(\mu)-(\bar{x}-\mu)^2} \tag{21}$$

$$\psi(\mu)=\Delta(\hat{\mu})+\Phi(\mu) \tag{22}$$

where $\bar{x}=\frac{1}{n}\sum_{i=1}^{n}|x_i|$. Then, the MLE values of the three SKL distribution parameters are obtained by,

$$\begin{aligned}\hat{\mu}&=x_i\\ \hat{\alpha}&=\frac{1}{2}\left(\Delta(\hat{\mu})-\bar{x}+\hat{\mu}+\Phi(\hat{\mu})\right)\\ \hat{\beta}&=\frac{1}{2}\left(\Delta((\hat{\mu}))+\bar{x}-\hat{\mu}+\Phi(\hat{\mu})\right)\end{aligned} \tag{23}$$

Appendix B The Standard Unit Commitment Formulation

B.1. Objective and Cost Functions

The total cost of generation for generator *i* can be obtained by summing the generator's production, start up and shut down costs, as shown in (24).

$$C_{g_{it}} = u_{it}A_i + B_i g_{it} + C_{it}^{SU} + C_{it}^{SD} \tag{24}$$

A generator incurs start-up cost when turning on from an off state, and similarly incurs shut down costs when a generator shuts down from an on state. Start-up and shut-down costs are limited by associated parameters, SUC_i and SDC_i and can be expressed as follow by (25)-(26).

$$C_{i.t}^{SU} \geq SUC_i(u_{it} - u_{i(t-1)}) \tag{25}$$

$$C_{it}^{SD} \geq SDC_i(u_{i(t-1)} - u_{it}) \tag{26}$$

The total cost for all generators is obtained by summing over all generators and time periods,

$$C = \sum_{i,t}(C_{g_{it}})$$

Then, the objective function is to minimize the cost of total generation.

B.2. Minimum Up- and Down-Time Constraints

The required parameters are as follows:

u_{i0}	Generator *i* commitment state during period 0
UT_{i0}	Cumulative up-time of generator *i* at the end of period 0

DT_{i0} Cumulative down-time of generator *i* at the end of period 0

MUT_i Minimum up-time of generator *i*

MDT_i Minimum up-time of generator *i*

Additionally, we define $M_i = \min\{T, (MUT_i - UT_{i0})u_{i0}\}$ to specify the number of hours a unit must stay on starting following period 0. Then, the up-time constraints can be expressed as follows [16],

$$\begin{aligned}
&\sum_{j=1}^{M_i}\left(1-u_{ij}\right)=0\\
&\sum_{j=1}^{MUT_i} u_{ij} - MUT_i\left(u_{it}-u_{i0}\right)\geq 0; \qquad t=1, M_i=0,\\
&\sum_{j=1}^{t+MUT_i-1} u_{ij} - MUT_i\left(u_{it}-u_{i(t-1)}\right)\geq 0; \quad t\neq 1, M_i+1\leq t\leq T-MUT_i+1,\\
&\sum_{j=1}^{T}\left(u_{ij}-u_{it}+u_{i0}\right)\geq 0; \quad t=1, T-MUT_i+2=1,\\
&\sum_{j=1}^{T}\left(u_{ij}-u_{it}+u_{i(t-1)}\right)\geq 0; \quad t\neq 1, T-MUT_i+2\leq t\leq T.
\end{aligned} \tag{27}$$

Similarly, for the down-time constraints, first we define $Q_i = \min\{T, (MUT_i - UT_{i0})u_{i0}\}$ to specify the number of hours a unit must stay off following period 0. Then, the up-time constraints can be expressed as follows [16],

$$\begin{aligned}
&\sum_{j=1}^{Q_i} u_{ij}=0\\
&\sum_{j=1}^{MDT_i}\left(1-u_{ij}\right) - MDT_i\left(u_{i0}-u_{it}\right)\geq 0; \qquad t=1, Q_i=0,\\
&\sum_{j=1}^{t+MDT_i-1}\left(1-u_{ij}\right) - MDT_i\left(u_{i(t-1)}-u_{it)}\right)\geq 0; \quad t\neq 1, Q_i+1\leq t\leq T-MDT_i+1,\\
&\sum_{j=1}^{T}\left(1-u_{ij}-u_{i0}+u_{it}\right)\geq 0; \quad t=1, T-MDT_i+2=1,\\
&\sum_{j=1}^{T}\left(1-u_{ij}-u_{i(t-1)}+u_{it}\right)\geq 0; \quad t\neq 1, T-MDT_i+2\leq t\leq T.
\end{aligned} \tag{28}$$

B.3. Hourly Generation and Ramp Constraints

u_{i0} Generator *i* commitment state during period 0

g_{i0} Power output of generator *i* during period 0

R_i^{up} Hourly ramp up limit of generator *i*

R_i^{dn} Hourly ramp down limit of generator *i*

R_i^{SU} Start-up ramp limit of generator *i*

R_i^{SDN} Shut-down ramp limit of generator *i*

The bounds on generation level from generator *i* at time *t* are,

$$g_i^{\min} u_{it} \le g_{it} \le g_i^{\max} u_{i,t};\ t = 1,...,T \tag{29}$$

The ramp up limits are as follows [14],

$$\begin{aligned} g_{it} &\le g_{i(t-1)} + R_i^{up} u_{i(t-1)} + R_i^{SU}\left(u_{it} - u_{i(t-1)}\right) + g_i^{\max}\left(1 - u_{it}\right);\ t = 2,...,T \\ g_{it} &\le g_{i0} + R_i^{up} u_{i0} + R_i^{SU}\left(u_{it} - u_{i0)}\right) + g_i^{\max}\left(1 - u_{it}\right);\ t = 1 \end{aligned} \tag{30}$$

The ramp down limits are as follows [16],

$$\begin{aligned} g_{it} &\ge g_{i(t-1)} - R_i^{up} u_{it} - R_i^{SDN}\left(u_{i(t-1)} - u_{it}\right) - g_i^{\max}\left(1 - u_{i(t-1)}\right);\ t = 2,...,T \\ g_{it} &\ge g_{i0} - R_i^{up} u_{it} - R_i^{SDN}\left(u_{i0} - u_{it}\right) - g_i^{\max}\left(1 - u_{i0}\right);\ t = 1 \end{aligned} \tag{31}$$

B.4. Demand and Generation Balance

Supple must meet the total demand minus the wind forecast,

$$\sum_i g_{it} = d_t - w_t^g \tag{32}$$

Where the generated wind is the net of forecasted wind, w_g minus the curtailed wind, w_g

$$w_t^g = w_t^f - w_t^s \tag{33}$$

There must also be enough reserve to meet up and down imbalances,

$$\begin{aligned} \sum_i g_{it} + \sum_i r_{it}^{up} &= d_t - w_t + err_t^{up} \\ \sum_i g_{it} - \sum_i r_{it}^{up} &= d_t - w_t - err_t^{up} \end{aligned} \tag{34}$$

Generation plus reserve must not exceed the maximum or minimum ramp capacity,

$$\begin{aligned} 0 \le r_{it}^{up} &\le r_{it}^{up\_\max} u_{it} \\ 0 \le r_{it}^{dn} &\le r_{it}^{dn\_\max} u_{it} \end{aligned} \tag{35}$$

References

[1] Global Wind Energy Council. (2014, Apr.). Global Wind Report 2013, [Online]. Available: http://www.gwec.net/publications/global-wind-report-2/

[2] B. Parsons, M. Milligan, B. Zavadil, D. Brooks, B. Kirby, K. Dragoon, and J. Caldwell, "Grid impacts of wind power: a summary of recent studies in the United States," *Wind Energy*, vol. 7, pp. 87-108, 2004.

[3] M. A. Ortega-Vazquez and D. S. Kirschen, "Assessing the Impact of Wind Power Generation on Operating Costs," *IEEE Transactions on Smart Grid*, vol. 1, pp. 295-301, 2010.

[4] R. Doherty; E. Denny, and M. O'Malley, "System operation with a significant wind power penetration," in *Power Engineering Society General Meeting*, June 2004.

[5] J. F. Restrepo and F. D. Galiana, "Assessing the Yearly Impact of Wind Power Through a New Hybrid Deterministic/Stochastic Unit Commitment," *IEEE Trans. Power Syst.*, vol. 26, pp. 401-410, 2011.

[6] F. Bouffard and M. Ortega-Vazquez, "The value of operational flexibility in power systems with significant wind power generation," in *Power and Energy Society General Meeting*, Detroit, MI, 2011.

[7] Erik Ela and J. Kemper, "Wind Plant Ramping Behavior," National Renewable Energy Laboratory, Tech. Rep., Boulder, CO, 2009.

[8] Bonneville Power Administration. (2011, Apr.). BPA balancing authority load and total wind generation: 2009. http://www.transmission.bpa.gov/Business/Operations/Wind/default.aspx."

[9] M. Milligan, E. Ela, D. Lew, D. Corbus, Y. Wan, and B. Hodge, "Assessment of Simulated Wind Data Requirements for Wind Integration Studies," *IEEE Transactions on Sustainable Energy*, vol.3, no.4, pp.620,626, Oct. 2012.

[10] NERC and CAISO, "2013 Special Reliability Assessment: Maintaining Bulk Power System. Reliability While Integrating Variable. Energy Resources – CAISO Approach", 2013. [Online]. Available: http://www.nerc.com/pa/RAPA/ra/Reliability%20Assessments%20DL/NERC-CAISO_VG_Assessment_Final.pdf

[11] M. S. Nazir, and F. Bouffard, "Intra-hour wind power characteristics for flexible operations," in *Power and Energy Society General Meeting*, San Diego, CA, July 2012.

[12] D. Milborrow. (2009, Jun.). Managing Variability. [Online]. Available: http://www.greenpeace.org.uk/files/pdfs/climate/wind-power-managing-variability.pdf

[13] E. Lannoye, M. Milligan, J. Adams, A. Tuohy, H. Chandler, D. Flynn, and M. O'Malley, "Integration of variable generation: Capacity value and evaluation of flexibility," in *Power and Energy Society General Meeting*, Minneapolis, MN, 2010.

[14] B.C. Ummels, M. Gibescu, E. Pelgrum, W.L. Kling, and A.J. Brand, "Impacts of Wind Power on Thermal Generation Unit Commitment and Dispatch," *IEEE Transactions on Energy Conversion*, vol. 22, no. 1, pp. 44–51, 2007.

[15] J. Wood and B. F. Wollemberg, *Power Generation Operation and Control*, 2nd edition. John Wiley & Sons, New York, 1996.

[16] M. Carrión and J. M. Arroyo, "A computationally efficient mixed-integer linear formulation for the thermal unit commitment problem," *IEEE Trans. Power Syst.*, vol.21, no.3, pp.1371,1378, Aug. 2006.

[17] F. Bouffard and F. D. Galiana, "Stochastic Security for Operations Planning With Significant Wind Power Generation," *IEEE Trans. Power Syst.*, vol. 23, pp. 306-316, 2008.

[18] H. Louie, "Evaluation of probabilistic models of wind plant power output characteristics," in *Probabilistic Methods Applied to Power Systems (PMAPS), 2010 IEEE 11th International Conference on*, 2010, pp. 442-447.

[19] Botterud, J. Wang, V. Miranda, and R. Bessa, "Wind Power Forecasting in U.S. Electricity Markets," *The Electricity Journal*, vol. 23, pp. 71-82, 2010.

[20] P. Puig and M. A. Stephens, "Goodness of fit tests for the skew-Laplace distribution.," *Statistics and Operations Research Transactions*, vol. 31, pp. 45-54, 2007.

[21] S. Kotz., T. J. Kozubowski, and K. Podgórski, *The Laplace distribution and generalizations: A Revisit with Applications to Communications, Economics Engineering, and Finance*. Birkhäuser Boston, 2001.

[22] A. Botterud, A. Zhou, J. Wang, R. Bessa, H. Keko, J. Mendes, J. Sumaili, and V. Miranda, "Use of Wind Power Forecasting in Operational Decisions," Argonne National Laboratory, Tech. Rep., Sept. 2011.

[23] R. Doherty, E. Denny and M. O'Malley, "System operation with a significant wind power penetration," *Power Engineering Society General Meeting*, June 2004.

[24] M.A. Ortega-Vazquez and D.S. Kirschen, "Estimating the Spinning Reserve Requirements in Systems With Significant Wind Power Generation Penetration," *IEEE Trans. Power Syst.*, vol. 24, no. 1, pp. 114–124, 2009.

[25] M.A. Ortega-Vazquez and D.S. Kirschen, “Optimizing the spinning reserve requirements using a cost/benefit analysis,” *IEEE Trans. Power Syst.*, vol. 22, no. 1, pp. 24–33, 2007.

[26] A. Tuohy, E. Denny, and M. O'Malley, “Rolling Unit Commitment for Systems with Significant Installed Wind Capacity,” *2007 IEEE Lausanne Power Tech*, pp. 1380–1385, July 1–5, 2007.

[27] P.A. Ruiz, C.R. Philbrick, E. Zak, K.W. Cheung, and P.W. Sauer, “Uncertainty Management in the Unit Commitment Problem,” *IEEE Trans. Power Syst.*, vol. 24, no.2, pp. 642–651, 2009.

[28] J. M. Morales, A. J. Conejo, and J. Perez-Ruiz, "Economic Valuation of Reserves in Power Systems With High Penetration of Wind Power," *IEEE Trans. Power Syst.*, vol.24, no.2, pp.900,910, May 2009.

[29] General Electric. FlexEfficiency 50 Plant. [Online]. Available: http://docs.wind-watch.org/FlexEfficiency-50-Plant-eBrochure.pdf

[30] D. Taylor and A. Pasha, “Economic operation of fast starting-HRSGs”, June 2010. [Online]. Available: http://www.powermag.com/economic-operation-of-fast-starting-hrsgs/?pagenum=4

[31] Electric Power Research Institute, "Damage to Power Plants Due to Cycling," Tech. Rep. 1001507, CA, July 2001.

[32] J. Ford, J. Fernandes, A. Shibli, “Damage to Power Plant due to Cyclic Operation and Guidelines for Best Practices,” Tech. Rep. ETD-1096-gsp-81, April 2009.

[33] N. Troy, E. Denny, and M. O'Malley, "Base-Load Cycling on a System With Significant Wind Penetration," *IEEE Trans. Power Syst.*, vol. 25, pp. 1088-1097, 2010.

[34] J. K. Delson, "Thermal stress computation for steam-electric generator dispatch," *IEEE Trans. Power Syst.*, vol. 9, pp. 120-127, 1994.

[35] H. Matsumoto, Y. Sato, F. Kato, Y. Eki, K. Hisano, and K. Fukushima, "Turbine Control System Based on Prediction of Rotor Thermal Stress,", IEEE Transactions on Power Apparatus and Systems, vol. PAS-101, pp. 2504-2512, 1982.

[36] C. Wang and S. M. Shahidehpour, "Optimal generation scheduling with ramping costs," in *Proc. 1993 Power Industry Computer Application Conference*, pp. 11-17.

[37] C. Wang and S. M. Shahidehpour, "Ramp-rate limits in unit commitment and economic dispatch incorporating rotor fatigue effect," *IEEE Trans. Power Syst.*, vol. 9, pp. 1539-1545, 1994.

[38] N. Troy, D. Flynn, M. Milligan, and M. O'Malley, "Unit Commitment With Dynamic Cycling Costs," *IEEE Trans. Power Syst.*, vol. 27, no.4, pp.2196,2205, Nov. 2012.

[39] Matlab R2012 Documentation - Statistics Toolbox. Available: http://www.mathworks.com/help/toolbox/stats/ecdf.html

[40] J. Apt, "The spectrum of power from wind turbines," *Journal of Power Sources*, vol. 169, pp. 369-374, 2007.

[41] J. Mur-Amada and A. A. Bayod-Rujula, "Wind power variability model Part I - Foundations," in *9th International Conference on Electrical Power Quality and Utilisation*, 2007, pp. 1-6.

[42] J. Mur-Amada and A. A. Bayod-Rujula, "Characterization of Spectral Density of wind farm power output," in *9th International Conference on Electrical Power Quality and Utilisation*, 2007, pp. 1-6.

[43] W. Katzenstein, E. Fertig, and J. Apt, "The variability of interconnected wind plants," *Energy Policy*, vol. 38, pp. 4400-4410, 2010.

[44] G. B. Shrestha, S. Kai, and L. Goel, "Strategic self-dispatch considering ramping costs in deregulated power markets," *IEEE Trans. Power Syst.*, vol. 19, pp. 1575-1581, 2004.

[45] F. Kaminsky, R. Kirchoff, C. Syu, and J. Manwell, "A comparison of alternative approaches for the synthetic generation of a wind speed time series," *Journal of Solar Energy Engineering*, vol. 113, pp. 280–289.

[46] A. D. Sahin and Z. Sen, "First-order Markov chain approach to wind speed modelling," *Journal of Wind Engineering and Industrial Aerodynamics*, vol. 89, pp. 263–269, 2001.

[47] A. Shamshad, M. Bawadi, W. W. Hussin, T. Majid, and S. Sanusi, "First and second order Markov chain models for synthetic generation of wind speed time series," Energy, vol. 30, pp. 693–708, 2005.

[48] K. Brokish and J. Kirtley, "Pitfalls of modeling wind power using Markov chains," Power Systems Conference and Exposition, 2009. PSCE '09. IEEE/PES , vol., no., pp.1,6, 15-18 March 2009